Redox Biology 80 (2025) 103499

Contents lists available at ScienceDirect

Redox Biology

journal homepage: www.elsevier.com/locate/redox

Caffeine ameliorates metabolic-associated steatohepatitis by rescuing hepatic Dusp9

Xin Xin [a,b,c,2], Cheng Chen [b,1,2], Xiao Xu [a,b,c], Sheng Lv [a,b,c], Qinmei Sun [a,b,c], Ziming An [a,b,c], Yi Chen [d], Zhekun Xiong [e], Yiyang Hu [a,b,c,**], Qin Feng [a,b,c,f,3,*]

[a] Key Laboratory of Liver and Kidney Diseases (Ministry of Education), Shuguang Hospital Affiliated to Shanghai University of Traditional Chinese Medicine, Shanghai, China
[b] Institute of Liver Diseases, Shuguang Hospital Affiliated to Shanghai University of Traditional Chinese Medicine, Shanghai, China
[c] Shanghai Key Laboratory of Traditional Chinese Clinical Medicine, Shanghai, China
[d] Division of Hematology and Oncology, Department of Medicine, Columbia Stem Cell Initiative, Columbia University Irving Medical Center, New York, USA
[e] Department of Spleen, Stomach and Hepatobiliary, Zhongshan Hospital of Traditional Chinese Medicine, Zhongshan, China
[f] Central Laboratory, Shuguang Hospital Affiliated to Shanghai University of Traditional Chinese Medicine, Shanghai, China

ARTICLE INFO

Keywords:
Caffeine (CAFF)
Black coffee
Metabolic dysfunction-associated steatotic liver disease (MASLD)
Dual-specificity phosphatase 9 (Dusp9)
Liver fibrosis

ABSTRACT

Caffeine (CAFF) is abundant in black coffee. As one of the most widely consumed beverages globally, coffee has been the focus of increasing clinical and basic research, particularly regarding its benefits in alleviating metabolic dysfunction-associated steatotic liver disease (MASLD). However, the therapeutic effects of CAFF on metabolic-associated steatohepatitis (MASH) and the underlying mechanisms remain unclear. In this study, we demonstrated that CAFF potently reduced hepatic steatosis, inflammation, and early-stage liver fibrosis in MASH mice induced by prolonged (36 weeks) high-fat high-carbohydrate (HFHC) diets and high-fat diets combined with carbon tetrachloride (CCl_4) injections. By using multiple target-identifying strategies, including surface plasmon resonance (SPR), cellular thermal shift assay (CETSA), and drug affinity responsive target stability (DARTS) assay, we identified dual-specificity phosphatase 9 (Dusp9) as a key therapeutic target, which was diminished by HFHC but restored with CAFF treatment. Dusp9 knockdown *in vivo* and *in vitro* exacerbated glycolipid metabolism disorders and stunningly counteracted the systemic therapeutic effects of CAFF in the MASH models. In addition, CAFF inactivated the ASK1-p38/JNK, a downstream signaling pathway of Dusp9, which regulates inflammation and apoptosis. Our study highlights the multifaceted benefits of CAFF in treating MASH by rescuing hepatic Dusp9 expression, thereby reversing glycolipid metabolism disorders, liver inflammation, and fibrosis. These findings provide experimental evidence supporting the clinical and daily use of CAFF and black coffee in managing MASH patients.

1. Introduction

Metabolic dysfunction-associated steatotic liver disease (MASLD) has become a global liver disease, affecting nearly one-quarter of the adult population worldwide [1,2]. Metabolic dysfunction-associated steatohepatitis (MASH), formerly known as nonalcoholic steatohepatitis (NASH), is the progressive stage of MASLD. In addition to excessive fat accumulation in the liver, MASH is characterized by hepatocellular ballooning and liver inflammation, which can lead to liver fibrosis and cirrhosis, hepatocellular carcinoma (HCC), and ultimately death [1,3].

* Corresponding author. Key Laboratory of Liver and Kidney Diseases (Ministry of Education), Shuguang Hospital Affiliated to Shanghai University of Traditional Chinese Medicine, Shanghai, China.
** Corresponding author. Key Laboratory of Liver and Kidney Diseases (Ministry of Education), Shuguang Hospital Affiliated to Shanghai University of Traditional Chinese Medicine, Shanghai, China.
E-mail addresses: huyiyang@shutcm.edu.cn (Y. Hu), fengqin@shutcm.edu.cn (Q. Feng).
[1] Present address: Laboratory of Liver Diseases, National Institute on Alcohol Abuse and Alcoholism, National Institutes of Health, Bethesda, MD, USA.
[2] These authors contributed equally.
[3] Lead contract.

https://doi.org/10.1016/j.redox.2025.103499
Received 16 December 2024; Received in revised form 12 January 2025; Accepted 14 January 2025
Available online 22 January 2025

MASH is part of a multisystem disease and is strongly associated with type 2 diabetes mellitus (T2DM) [4,5]. These two diseases often coexist and synergistically increase the risk of adverse hepatic and extra-hepatic outcomes [4]. Hyperglycaemia and chronic hyperinsulinemia subsequently activate hepatic de novo lipogenesis (DNL), leading to exacerbating fatty acid biosynthesis and hepatic lipid accumulation [6–8].

Consumption of commercial sugar-sweetened beverages has been associated with increased incidence and mortality rates of various types of cancer [9]. However, the independent contribution of such beverages to the development of MASLD/MASH and their role in the daily management of MASLD/MASH patients has been largely overlooked. Beyond dietary and exercise guidance for MASLD patients, consuming healthy beverages such as black coffee, which contains multiple natural components including caffeine (CAFF), offers significant benefits to MASLD without any significant adverse effects [10]. Coffee is the most popular beverage in Western countries. Several epidemiological studies have indicated its beneficial effects in MASLD patients, including reduced risks of metabolic syndrome, diabetes, hepatic fibrosis, and even HCC [11–15]. Consistent with these clinical findings, our previous study highlighted the multiple therapeutic effects of caffeine on MASH mice, particularly in improving glycolipid metabolism and hepatic inflammation [16]. Although increasing clinical studies suggest the therapeutic effects of black coffee or caffeine consumption, limited basic research on the detailed mechanisms has left the clinical effects of coffee consumption obscure. Therefore, the specific potential mechanisms and therapeutic targets of caffeine in alleviating MASH need to be elucidated.

Dual-specificity phosphatase 9 (Dusp9), also known as MAP kinase phosphatases-4 (MKP-4), is a member of the DUSP protein family. It has been shown to inhibit insulin signal transduction and protect against the development of insulin resistance in T2DM [17,18]. Notably, Dusp9 has been further identified to exert hepatoprotective effects by directly suppressing apoptosis signal-regulating kinase 1 (ASK1) and its downstream kinases p38 and c-Jun *N*-terminal kinase (JNK) [19], making Dusp9 a promising target for the treatment of MASH [19,20].

The current study systematically mapped out the therapeutic effects of caffeine in treating MASH with early-stage liver fibrosis, comprising amelioration of glycolipid metabolism, and improvement of liver inflammation and fibrosis. Multiple target-identifying strategies highlighted the direct binding between CAFF and Dusp9, supporting that Dusp9 is a crucial therapeutic target of CAFF in treating MASH. By using Dusp9 knockout mice and Dusp9 silenced hepatocytes, we confirmed the contributions of the Dusp9 deficiency to the progression of MASH. More importantly, the beneficial effects of CAFF have been largely dismissed by Dusp9 knockdown *in vivo* and *in vitro*, confirming that Dusp9 is one of the key targets of caffeine in ameliorating MASH. Finally, these findings laid the foundation for the clinical and daily administration of caffeine-rich beverages, such as black coffee, for managing MASH patients with early-stage liver fibrosis.

2. Results

2.1. Caffeine attenuates hepatic lipid accumulation and improves systemic lipid and glucose metabolism in HFHC-induced MASH mice

To generate the MASH phenotype, mice were consistently fed a high-fat high-carbohydrate (HFHC) diet for 36 weeks. To further study the effects of caffeine (CAFF) on MASH, these mice were administered (by gavage) with or without CAFF-contained drinking water during the final 6 weeks (Fig. 1A). In agreement with our previous study [16,21], and as illustrated in Fig. 1B, the long-term HFHC diet led to significant body weight gain. Compared with HFHC mice, CAFF markedly reduced the body and liver weight (Fig. 1B, C, 1D), this may be due to the declined food intake (Sup Fig. 1A). In addition, the liver/body weight ratio and spleen weight were significantly decreased following CAFF treatment (Sup Fig. 1B and C). In HFHC mice, the hepatocytes were filled with lipids, as shown by Oil-red O staining (Fig. 1B), and liver triglyceride (TG) was quantified about 2.5 folders more than the normal level (Fig. 1E). However, hepatic lipid accumulation was significantly ameliorated by CAFF treatment (Fig. 1B, E,1F). Moreover, CAFF substantially improved systemic lipid metabolism, including reducing serum TG (Fig. 1G), TC (Fig. 1G), and LDL (Fig. 1H) levels. It is notable that glucose metabolism disorders and insulin resistance typically coexist in MASH patients [4,8,22]. Consistent with this, the HFHC diet largely increased fasting plasma glucose (FBG) and serum insulin (FINS) levels (Fig. 1I), leading to a high HOMA-IR index (Fig. 1J). Nevertheless, CAFF demonstrated robust effects in normalizing disordered glucose and insulin levels (Fig. 1I and J).

Consistent with our previous data [16], CAFF administration strongly suppressed hepatic *Srebp1c, Fasn, Acc,* and *Scd*-1 mRNA expression (Fig. 1K), indicating a suppression of the de novo lipogenesis (DNL) process in the MASH liver [6,7]. Conversely, *Cpt-1*, the key shuttle protein located in the outer mitochondrial membrane [23], was upregulated (Fig. 1K), which may enhance the fatty acid oxidation in mitochondria. In addition, *fabp-1* and *Cd36*, which are important fatty acid-binding proteins and lipid membrane transporter that facilitate free fatty acid (FFA) uptake [24–26], were sharply downregulated following CAFF treatment (Fig. 1K). Meanwhile, *ChREBP* and *G6Pase*, genes involved in regulating glucose and fructose response, were significantly suppressed by CAFF [27,28] (Fig. 1L).

To determine whether CAFF has direct effects on lipid metabolism in the hepatocyte, THLE-2 cells (human liver cell line) [29] were loaded with FFAs and subsequently co-incubated with three concentrations of CAFF (Fig. 1M). In line with the reduction in intracellular lipid accumulation (Fig. 1N, Sup Fig. 1D), TG levels decreased in a dose-dependent manner following CAFF treatment (Fig. 1O), which was accompanied by a significant downregulation of DNL genes (*Srebp1c, Fasn, Acc,* and *Scd-1*), lipid binding and transportation genes (*Fabp-1*, *Cd36*), and an upregulation of the lipid oxidation gene (*Cpt1*) (Fig. 1P).

2.2. Caffeine reverses steatohepatitis and liver fibrosis in HFHC-induced MASH mice and a liver fibrosis model mediated by a high-fat diet combined with CCl_4 injections

The presence of macrosteatosis with inflammatory infiltrates in the liver due to the HFHC diet was reconfirmed by liver H&E staining (Fig. 2A). Ballooning hepatocytes were filled with lipids which push the nucleus to the side. In contrast, CAFF administration enormously attenuated steatosis and inflammatory infiltrates in the hepatocytes (Fig. 2A). The MASLD activity score including steatosis, ballooning, inflammation, and MAS score were all improved in the CAFF group (Fig. 2B, Sup Fig. 1D, E, F). Moreover, the elevated serum ALT and AST activities in HFHC mice were reversed by CAFF treatment, indicating an amelioration in liver injury (Fig. 2C). F4/80, a marker of macrophages, was highly expressed in HFHC mice, suggesting macrophage infiltration in the liver (Fig. 2A). In addition, except *Il6*, genes associated with macrophage recruitment and inflammation (*Tnfα, Il1β, Ccl2, Ccl5, Cxcl2, Cxcl10*) were strongly suppressed by CAFF (Fig. 2D) [30–32], explaining the reduced presence of macrophages in the CAFF group (Fig. 2A). This suppression on inflammatory genes was also observed in FFAs-loaded THLE-2 hepatocytes (Sup Fig. 2A).

Further studies employed Picro Sirius Red (PSR) and Masson's trichrome staining, combined with hepatic stellate cell (HSC) makers α-SMA and collagen-1 (Col-1) staining (Fig. 2E). As illustrated in Fig. 2E, a large fibrosis area was indicated by PSR and Masson staining in the HFHC group, corresponding to a marked elevation in collagen and HSCs expression, indicating the progression of liver fibrosis in MASH mice. Along with reduced liver inflammation, CAFF also largely reversed liver fibrosis (Fig. 2E, F, 2G). Hydroxyproline, a major component of collagen, has been reported to be highly correlated with HCC progression in the MASH model [33]. In this study, liver HYP content was doubled by the HFHC diet but decreased with CAFF administration

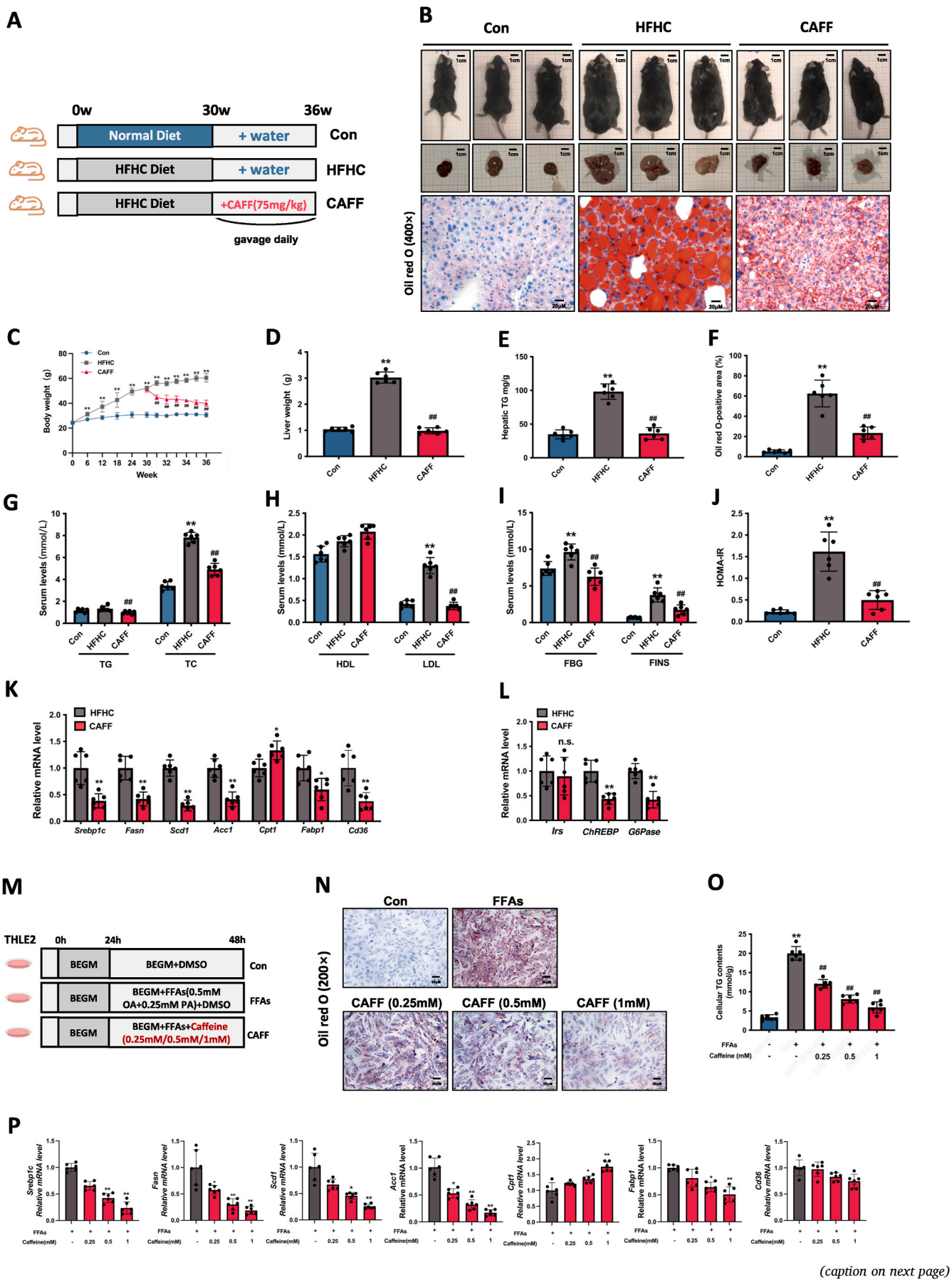

(caption on next page)

Fig. 1. Caffeine administration ameliorates liver steatosis in HFHC-fed MASH mice. (A) Experimental design illustrating the experimental flow. Mice were fed a normal diet (control, Con) or HFHC diet for 36 weeks to induce MASH, with or without caffeine administration by oral gavage in the last 6 weeks (n = 6). (B) Representative images showed gross body, liver morphology, and Oil Red O staining of mouse livers. (C, D) Body weight and liver weight. (E) Hepatic TG contents (mg/g). (F) Quantification of Oil red O staining. (G, H) Levels of serum TG, TC, HDL, and LDL indexes. (I, J) Fasting plasma glucose, fasting insulin, and insulin resistance index, HOMA-IR (homeostasis model assessment). (K) Quantitative PCR was performed to determine the hepatic mRNA levels of genes related to lipid metabolism (*Srebp1c*, *Fasn, Scd1*, *Acc1*, *Cpt1a*, *Fabp1,* and *Cd36*). (L) Quantitative PCR was performed to determine the hepatic mRNA levels of genes related to glucose metabolism (*Irs*, *ChREBP,* and *G6Pase*). (M) Flow chart of the cell culture experimental design. THLE-2 cells were stimulated with FFAs and co-treated with caffeine (0.25, 0.5, and 1 mM) for 24 h. The experiment was repeated three times. (N) Representative images showing Oil red O staining and semi-quantitative assessment of Oil red O content. Scale bar, 20 μm (n = 3 independent experiments per group) (O) Levels of intracellular TG. (The data were obtained from three independent experiments per group) (P) Quantitative PCR was performed to determine the THLE-2 cells mRNA levels of genes related to lipid metabolism (*Srebp1c*, *Fasn, Scd1*, *Acc1*, *Cpt1a*, *Fabp1,* and *Cd36*). Data are presented as the mean ± SD. Significant differences between the Con group and the HFHC group, $*p < 0.05$, $**p < 0.01$; the significant difference between the HFHC group and the caffeine group, $\#p < 0.05$, $\#\#p < 0.01$. The data were analyzed with a two-sided Student's t-test or one-way ANOVA.

(Fig. 2H). Furthermore, HSCs activation and fibrogenic genes (*α-SMA, Cola1, Cola3, Tgf-β,* and *Timp-1*) were dramatically downregulated by CAFF treatment (Fig. 2I).

To further explore the anti-fibrosis effects of CAFF, we used a 6-week HFHC combined with CCl_4 injection to induce fibrosis in a fatty liver model (Fig. 2J). Intriguingly, CCl_4 triggered declining body weight, but the liver weight **(Sup** Fig. 2B and C) was comparable among the three groups. Still, liver injury indexes (ALT, AST) (Fig. 2K), hepatic lipid accumulation (hepatic TG) **(Sup** Fig. 2D), and liver HYP content **(Sup** Fig. 2E) were undoubtedly reduced by CAFF administration. As illustrated by H&E and PSR staining (Fig. 2L), liver lipid contents and fibrosis were markedly decreased with CAFF treatment, strongly supporting the anti-fibrosis effect of CAFF treatment.

2.3. CAFF directly binds hepatic Dusp9 for treating MASH

To identify the potential target of CAFF in alleviating MASH, we utilized transcriptomics computational biology, systems pharmacology technology, and a detailed screening process as outlined in Fig. 3A. We conducted transcriptome analysis on mouse liver tissues following CAFF intervention. The PCA results revealed significant differences between the two groups (n = 4) with each group showing good internal consistency **(Sup** Fig. 3A). Subsequently, Gene Set Enrichment Analysis (GSEA) indicated the significantly altered pathways, which could be categorized into three major groups: glucose and lipid metabolism, inflammation, and fibrosis **(Sup** Fig. 3B, C, D). We identified potential CAFF drug targets using the PharmMapper database, while MASH-related targets were obtained from the GeneCards database. The intersection of CAFF and MASH target genes revealed 11 common genes, with Dusp9, Col1a1, Ccl2, and Cd68 being closely associated with MASH **(Sup** Fig. 3E). Molecular docking studies suggested that CAFF has the highest affinity for Dusp9, with the binding site located in the active pocket, potentially affecting its dephosphorylation capacity (Fig. 3B). Thereafter, several validation experiments are performed to verify the interaction between CAFF and Dusp9.

By using surface plasmon resonance (SPR), which is an optical technique used to measure molecular interactions in real time [34], CAFF was proved to have a direct binding with Dusp9 in a dose-dependent manner, and the K_D value is 1.860E-4 (mol/L) (Fig. 3C and D). CESTA and DARTS are techniques that assess the thermal stability of proteins upon ligand binding [35]. These methods are commonly employed to investigate the direct pharmacological targets of compounds, as ligand binding can either enhance or reduce the thermal or protease stability of proteins. The CESTA results showed that Dusp9 expression in the CAFF-treated group was significantly higher than in the non-CAFF-treated group (Fig. 3E and F), indicating that CAFF increased the thermal stability of Dusp9. Additionally, the DARTS assay demonstrated that Dusp9 expression increased linearly with CAFF concentration in the presence of a protease, suggesting that CAFF enhances the enzymatic stability of Dusp9 (Fig. 3G and H). Collectively, these results strongly support that CAFF binds directly with Dusp9.

To confirm the effects of CAFF on the regulation of Dusp9 in MASH models, the liver Dusp9 protein expression was detected by Western Blotting and liver section staining. As shown in Fig. 3I 3J, CAFF markedly reversed the suppressed Dusp9 protein expression in the MASH liver. Additionally, Fig. 3M illustrated that Dusp9 expression in the cytoplasm of hepatocytes was dramatically decreased in the HFHC mice. However, abundant Dusp9-positive stained hepatocytes were observed after CAFF treatment. Furthermore, CAFF exhibited direct effects on increasing Dusp9 expression in a dose-dependent manner in the FFA-incubated THLE-2 cell line (Fig. 3K and L).

As shown in Fig. 4A, Dusp9 was proven to prevent MASH progression by dephosphorylating and inactivating specific kinases such as ASK1 (apoptosis signal-regulating kinase 1), p38 (protein kinases activated by stress), and JNK (c-Jun *N*-terminal kinases) [19,20]. These kinases play important roles in promoting lipotoxicity, hepatic inflammation, and fibrosis, which are all implicated in the development of MASH [36,37]. Therefore, we assessed the phosphorylation levels of ASK-1, p38, and JNK in the liver. As shown in Fig. 4B and C, the phosphorylation levels of the ASK1-p38/JNK signaling pathway were strongly induced by the HFHC diet, but undoubtedly impaired by CAFF administration, which further explains the improvement in liver inflammation and fibrosis due to the CAFF intake. The same results were replicated in THLE-2 cells, where CAFF inactivated the ASK1-p38/JNK signaling pathway in a dose-dependent manner (Fig. 4D and E).

2.4. Dusp9 knockdown aggravates MASH development and blunts the therapeutic effects of caffeine in MASH mice

Considering the direct binding of CAFF with Dusp9 and the multiple roles of Dusp9 in improving glucose and lipid metabolism, as well as alleviating liver inflammation in MASLD mice [19]. We speculated that Dusp9 could be a therapeutic target of CAFF in treating MASH. To verify that, after 26 weeks on an HFHC diet, 16 MASH mice were intravenously injected with adeno-associated virus 2/8 (AAV2/8) to mediate liver-specific Dusp9 knockdown. The efficiency of AAV2/8-mediated Dusp9 knockdown was confirmed by protein expression analysis **(Sup** Fig. 4A and B). Compared to the control virus group, 4 weeks of Dusp9 knockdown further increased body weight ($p = 0.0299$) **(Sup** Fig. 4C). Additionally, liver TG accumulation was enhanced by Dusp9 knockdown (n = 3) **(Sup** Fig. 4D), indicating the contribution of Dusp9 deficiency to the progression of MASH.

To further confirm whether CAFF ameliorates the MASH phenotype via Dusp9 and its tightly regulated downstream signals, half of Dusp9 knockdown mice were treated with CAFF for an additional 6 weeks (Fig. 5A). Although the CAFF administration markedly reduced body and liver weight, this effect was significantly blunted by Dusp9 knockdown (Fig. 5B and C, Sup 5A). Of note, Dusp9 knockdown increased food intake, compared with the HFHC control group (Sup Fig. 5B). By contrast, CAFF presented powerful suppression of HFHC food intake in control and Dusp9 knockdown mice (Sup Fig. 5B), which explains the decreasing body and liver weight after CAFF administration. Water consumption showed no difference among four groups (Sup Fig. 5C). As illustrated in Fig. 5D and Sup Fig. 5D (Oil red O and H&E staining) and

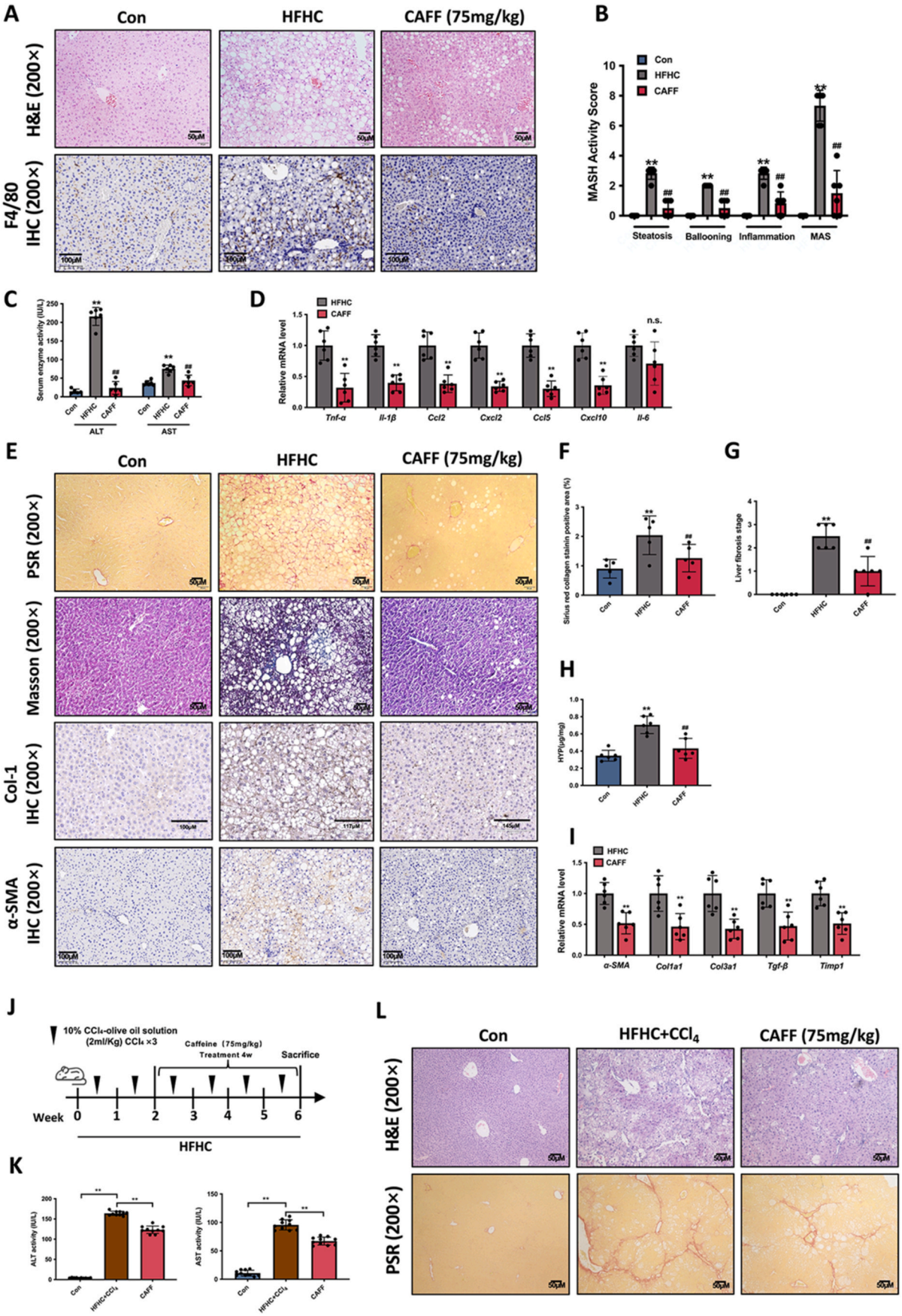

(caption on next page)

Fig. 2. Caffeine administration mitigates liver inflammation and fibrosis in MASH mice. (A) Representative images showed liver tissue H&E staining and F4/80 IHC staining (200 × magnification). (B) Hepatic ballooning, steatosis, lobular inflammation, and MASH score (MASH activity score). (C) Serum ALT and AST activities. (D) Quantitative PCR was performed to determine the hepatic mRNA levels of inflammation-related genes (*Tnf-α, Il-1β, Ccl2, Cxcl2, Ccl5, Cxcl10,* and *Il-6*). (E) Representative images of PSR, Masson, Col-1 IHC, and α-SMA IHC stained liver sections, PSR quantification is provided in (F). (G) Liver fibrosis stage in mice from each group according to PSR staining. (H) Hydroxyproline content of liver tissue in each group. (I) Quantitative PCR was performed to determine the hepatic mRNA levels of genes related to fibrosis (*α-SMA, Cola1, Cola3, Tgf-β,* and *Timp1*) from the indicated groups. (J) Working flow of liver fibrosis mice model. Mice were fed with a control diet (Con) or high-fat diet (HFHC) for 6 weeks, HFHC mice were consistently intraperitoneally injected with CCl_4, 3 times per week. In the last 4 weeks, half of the HFHC mice were treated with CAFF. (K) Serum ALD and AST activities. (L) Representative Liver H&E staining, and PSR staining in three indicated groups. Data are presented as the mean ± SD. The significant difference between the Con group and the HFHC group, n = 6, $*p < 0.05$, $**p < 0.01$; significant differences between the HFHC group and the caffeine group, $\#p < 0.05$, $\#\#p < 0.01$. The data were analyzed with a two-sided Student's t-test or one-way ANOVA.

TG content measurement (Fig. 5E), the reduction in hepatic fat accumulation due to the CAFF consumption was stunningly counteracted by the Dusp9 knockdown. Similar impairing effects due to Dusp9 knockdown among the CAFF treatment groups were also observed in serum TG, TC, and LDL-C levels (Sup Fig. 5E, F, G).

In agreement with previous studies, Dusp9 deficiency is a high-risk factor for insulin resistance (IR) [17,18]. The exacerbated serum insulin levels (Fig. 5G) and IR (Fig. 5H) triggered by Dusp9 impairment were observed in the HFHC group. Moreover, Dusp9 knockdown further impaired the beneficial effects of CAFF on FBG, FSI, and HOMA-IR indexes (Fig. 5F, G, 5H), highlighting that Dusp9 is a critical target of CAFF in normalizing glucose metabolism in the MASH model. Although similar activities of ALT and AST (Fig. 5I and J), NAS score (Fig. 5K), HYP content (Fig. 5L), and PSR staining (Fig. 5M) were observed in Dusp9 knockdown mice with HFHC feeding, indicating that Dusp9 impairment did not exacerbate liver inflammation and fibrosis, Dusp9 knockdown strongly impaired the effects of CAFF in ameliorating these liver indexes. Taken together, Dusp9 is a critical target of CAFF in treating MASH, which deficiency leads to glucose and insulin metabolism disorders and ultimately contributes to MASH progression.

2.5. The anti-inflammatory and anti-fibrotic effects of CAFF on MASH mice largely depend on liver Dusp9 expression and its downstream singling

Next, the major downstream signals, ASK1-p38/JNK, and their phosphorylation proteins were examined by western blotting. As expected, CAFF strongly induced the liver Dusp9 expression (Fig. 6A and B) which subsequently impaired the phosphorylation of ASK1-p38/JNK signaling (Fig. 6A and B). However, these effects of CAFF treatment were significantly reversed in the absence of Dusp9, ultimately exacerbating the MASH progress. As illustrated in Dusp9 staining (Fig. 6C), the upregulated liver Dusp9 expression induced by CAFF was completely suppressed by Dusp9 knockdown. Consequently, the reduction in F4/80 and α-SMA expression observed in the CAFF treatment group was partially reversed in the Dusp9 knockdown group (Fig. 6C). Specifically, more F4/80-stained macrophages were observed near the portal area and increasing α-SMA-stained HSCs were detected adjacent to the macro lipid droplets, indicating hepatic inflammation and fibrosis.

In line with the exacerbation of liver inflammation and fibrosis, the hepatic lipogenesis and fatty acid oxidation-related genes (*Srebp1c, Fasn, Acc, Scd-1*, and *Cpt-1*) normalized by CAFF were reversed in the Dusp9-deficient group (Fig. 6D), explaining the re-accumulation of hepatic lipids despite CAFF administration. Additionally, liver inflammatory and necrotic genes (*Tnfα, Il1β, Ccl2, Cxcl2, Ccl5*) were restored (Fig. 6E) in the absence of Dusp9, highlighting the worsening liver injury. Consistently, the suppression of HSCs activation and fibrosis-related genes (*α-SMA, Cola1, Cola3, Tgf-β)* by CAFF was also reversed (Fig. 6F).

Taken together, Dusp9 is a critical target of CAFF in ameliorating MASH progress. Dusp9 knockdown proportionally diminished the improvements in liver energy metabolism, inflammation, and fibrosis induced by CAFF consumption, which were highly attributed to the activation of ASK1-*p*38/JNK signaling and restored genes expression related to DNL, liver inflammation, and fibrosis.

2.6. Dusp9 deficiency impairs CAFF-mediated hepatic lipids elimination and restores DNL and inflammatory gene expression in vitro

Next, we investigated whether CAFF directly affects hepatic lipid and inflammation regulation via Dusp9. As shown in Fig. 7A, Dusp9 silencing in THLE-2 cells was achieved using shRNA, followed by co-incubation with FFAs in the presence and absence of CAFF. The efficiency of shRNA knockdown was confirmed by GFP fluorescence and WB detection **(Sup** Fig. 6A). Consistent with our results above, hepatic lipid accumulation due to the FFAs incubation was dramatically decreased by CAFF treatment. However, this reduction was notably diminished by Dusp9 knockdown (Fig. 7B, C, 7D), supporting a direct ameliorating effect by CAFF on lipid metabolism in hepatocytes. Although CAFF treatment suppressed the phosphorylation of the ASK-*p*38/JNK signaling pathway, silencing Dusp9 restored the activation of the ASK-*p*38/JNK pathway, regardless of CAFF interference (Fig. 7E), which leads to the increased lipid accumulation and inflammatory gene expression in hepatocytes. Similarly, in line with *in vivo* results, CAFF-mediated suppression on hepatic DNL genes (*Srebp1, Fasn, Acc, Scd-1*) (Fig. 7F) and inflammatory genes (*Tnfα, Il1β, Ccl2, Cxcl2*) was reversed in Dusp9-deficient hepatocytes, explaining the re-emergence of hepatic steatosis and inflammation (Fig. 7G).

In summary, this study demonstrates that Dusp9 is a key therapeutic target rescued by caffeine administration, which further suppresses ASK-p38/JNK downstream signaling activation and related gene dysregulation. These beneficial effects contribute to the significant therapeutic outcomes of caffeine, including the attenuation of hepatic lipid accumulation and the reversal of liver inflammation and fibrosis, thereby ameliorating the progression of MASH (Fig. 8).

3. Discussion

In the current study, we first systematically outlined the metabolic benefits of caffeine (CAFF) consumption in two types of experimental MASH models, including long-term (36 weeks) HFHC-induced MASH models, and the HFHC diet cooperated with CCl_4 injection-induced MASH model with liver fibrosis. Furthermore, hepatic Dusp9 was identified as the therapeutic target of CAFF in ameliorating liver steatosis, inflammation, and fibrosis. In addition, the downstream signaling of Dusp9 was involved in CAFF-mediated improvements in MASH.

The quest for efficient therapies has become an urgent focus in MASLD research over the past decades. Recently, resmetirom (rezdiffra) was approved by the U.S. Food and Drug Administration for treating adults with noncirrhotic MASH with moderate to advanced liver scarring (fibrosis), to be used alongside diet and exercise [38–40]. However, daily management, including moderate exercise, and healthy food and beverage consumption, remains the cornerstone of MASLD management. Sugar-sweetened beverages were identified by a meta-analysis to have a positive significant association with MASLD in both men and women [41], highlighting the essentials of drinking healthy beverages. Black coffee is the most frequently consumed CAFF-containing beverage, which presents multiple beneficial effects on health [42]. Epidemiological data and meta-analysis in humans have provided compelling evidence that coffee and CAFF are beneficial in improving MASLD/MASH [12,15,43,44]. Similar to most drugs in clinical trials

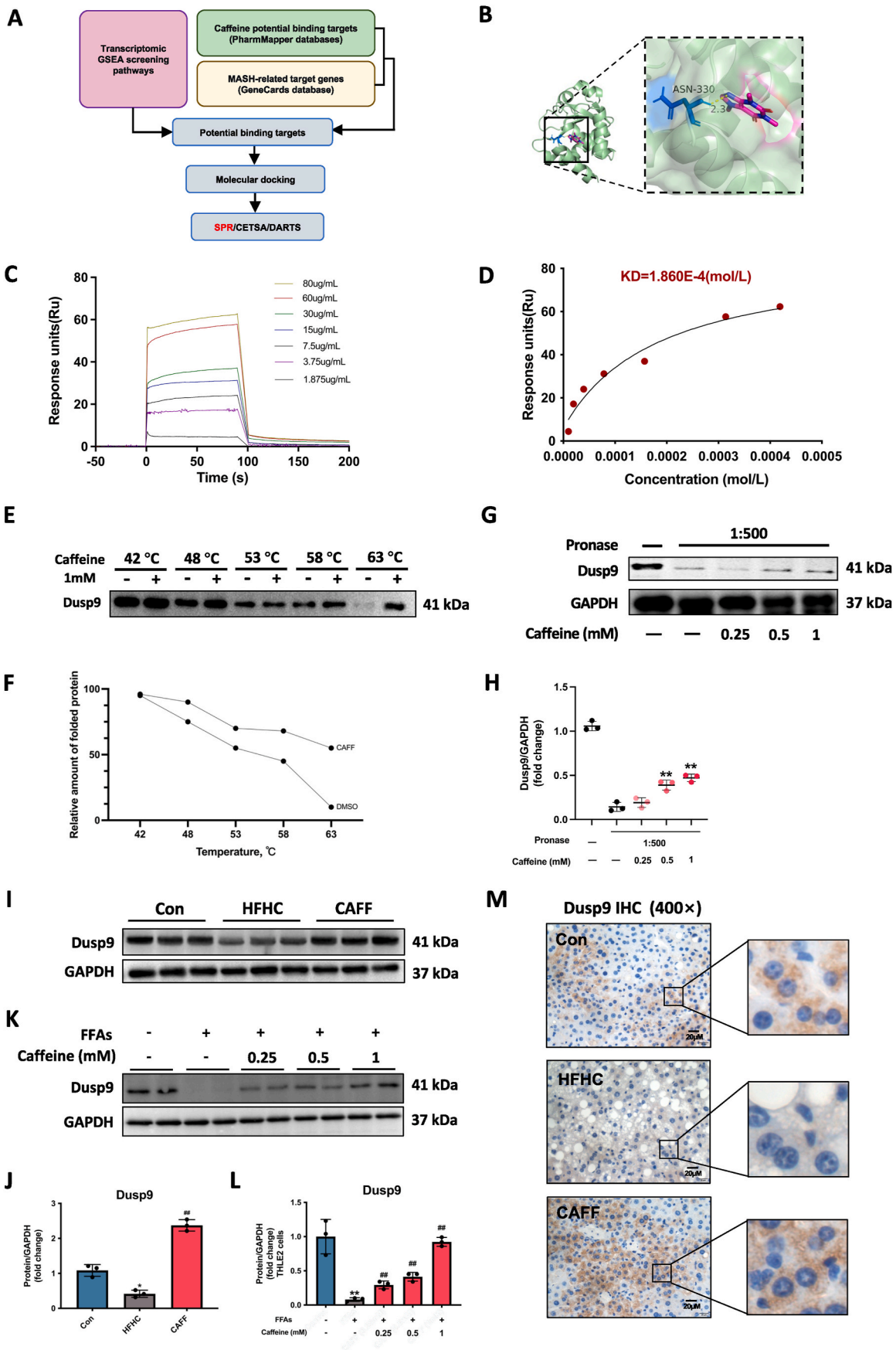

(caption on next page)

Fig. 3. Screening, prediction, and validation of caffeine directly targets Dusp9. (A) Workflow for identifying potential drug targets of caffeine. (B) Molecular docking of caffeine with the protein Dusp9. (C, D) The affinity of CAFF for Dusp9 was determined by using SPR. (E) Representative immunoblots from (Cellular Thermal Shift Assay) CETSA experiments in THLE-2 cells (42/48/53/58/63 °C). (F) Melt curves of Dusp9 in THLE-2 cells after caffeine or DMSO treatment by CETSA. (G) Drug affinity responsive target stability (DARTS) assay was performed to test the direct binding of Caffeine to Dusp9. (H) Fold change of Dusp9 in THLE-2 cells after caffeine (0.25/0.5/1 mM) or DMSO treatment by DARTS. (I) Expression levels of hepatic Dusp9 protein were examined with Western blot in HFHC MASH mice. (J) Western blot data of relative expression of Dusp9 protein in HFHC MASH mice. GAPDH served as a loading control. (n = 3 per group). (M) Immunohistochemical detection of Dusp9 (brown/tan) and nuclei (blue) in liver tissue from HFHC-fed MASH mice. (K) Western blot data of relative expression of Dusp9 protein in FFA-induced THLE-2 cells. (L) Relative levels of Dusp9 were analyzed in THLE-2 cells. Experiments were performed three times independently, and values represent means ± SD.*, compared with Con $p < 0.05$; **, compared with Con $p < 0.01$; #, compared with HFHC $p < 0.05$; ##, compared with HFHC $p < 0.01$. The data were analyzed with a two-sided Student's t-test or one-way ANOVA.

targeting MASLD/MASH, which significantly suppress food intake and decrease body weight (e.g., GLP-1 receptor agonists) [45], CAFF has shown remarkable experimental effects on normalizing body weight after even one week of oral administration in our study. These effects of CAFF in the MASH mice model align with clinical observations that high CAFF intake is associated with body weight loss through thermogenesis and fat oxidation [46]. Importantly, liver weight was dramatically reduced, accompanied by robust histological improvements, including reduced hepatic steatosis, inflammation, and fibrosis due to the CAFF consumption, underscoring the multi-therapeutic effects of CAFF in alleviating MASH. Additionally, consistent with clinical data from decades ago [47], fasting blood glucose and insulin levels in the MAHS mice were significantly normalized by CAFF intake in the current study, supporting that CAFF improves glucose metabolism and further ameliorates T2MD. Given the interaction between MASLD and T2MD in the pathogenesis of intrahepatic and extrahepatic glycolipid metabolism, CAFF consumption greatly improves both conditions, ultimately contributing to the amelioration of liver metabolism disorders. However, the clinical effects of CAFF intake or coffee consumption in treating MASLD remain controversial. Only CAFF intake from regular coffee was reported to be efficient for hepatic fibrosis amelioration in MASLD patients [43,44]. One clinical research with relatively fewer patients was against the effects of CAFF on the improvement of the liver condition in MASLD patients [48]. These negative outcomes might be due to the limited number of patients and lower daily consumption of CAFF (200 mg). One recent study indicates that high coffee consumption (≥3 cups daily) was inversely related to MASLD prevalence, with an adjusted odds ratio of 0.35 (95 % CI: 0.14–0.89) [49]. Consistent with this finding, Chen et al. provided a meta-analysis results in 2019: Coffee intake level more than 3 cups was observed lower risk of MASLD than <2 cups per day [50], suggesting the dose-dependent manner of coffee consumption in preventing MASLD. Further trials with higher dosages, and longer duration are highly recommended.

Dusp9 has been elucidated to negatively regulate insulin resistance [17,51] and enzymes involved in gluconeogenesis and lipogenesis, such as fructose-1,6-biphosphatase, SREBP-1C, SCD-1, and ACC, which are critical for the progression of MASLD [51]. Our unpublished data showed that CAFF intervention can rescue suppressed hepatic Dusp9 in MASH mice, which may imply the mechanism by which CAFF ameliorates experimental MASH. Here, in these 36-week HFHC-induced MASH mice, hepatic Dusp9 expression was reconfirmed to be suppressed by the HFHC diet but was stunningly rescued by CAFF treatment, supporting our hypothesis that reversing suppressed Dusp9 is a critical mechanism by which CAFF alleviates MASH. Except for Dusp9, several genes were highlighted as being regulated by CAFF by GSEA assay. However, by using SPR, CETSA, and DARTS assays, multiple methods helping to evaluate drug-binding to the target protein, we confirmed that CAFF has a direct and stable binding with Dusp9 in a dose-dependent manner, strongly indicating that Dusp9 is a potent target of CAFF. Finally, in the Dusp9 knockdown mice, the fasting insulin level and HOMA-IR were stunningly increased, which agrees with the regulation of Dusp9 on insulin level and glucose metabolism. Moreover, the impaired improvements of glycolipid metabolism and restoration of genes related to de novo lipogenesis (*Srebp-1c*, *Scd-1*, and *Acc*) due to Dusp9 knockdown in the CAFF treatment group strongly support the fact that CAFF ameliorates glycolipid metabolism disorder in MASH through rescuing hepatic Dusp9. Consistent with our *in vivo* data, lipid accumulation and lipid synthesis genes in FFA-treated hepatocytes were largely blunted in line with escalating dosages of CAFF intervention, but reversed by Dusp9 silencing, which demonstrates the interaction of CAFF with Dusp9 for ameliorating lipid metabolism in hepatocytes.

Liver inflammation and early stage of liver fibrosis are hallmark features of MASH, often accompanied by macrophage infiltration and hepatic stellate cell activation [52]. In our study, CAFF was confirmed to exhibit anti-inflammation and anti-fibrosis effects demonstrated by ameliorated MASLD score, improved pathological staining (PSR and Masson staining), and lower HYP content in two independent HFHC-induced MASH models. Additionally, the high-fat diet combined with the carbon tetrachloride (CCl_4) injection model emphasized the anti-fibrosis effect of CAFF in the liver and supported that CAFF protects mice against liver fibrosis not only developed by long-term HFHC diet but also induced by chemistries, which is consistent with several published studies [13,53,54]. Meanwhile, $F4/80^+$ macrophage infiltration and HSC activation were largely reversed by CAFF administration, in line with downregulated inflammatory and fibrogenic genes, highlighting the alleviation in liver inflammation and fibrosis by CAFF administration.

Dusp9 deficiency was first reported by Ye et al. to aggravate hepatic steatosis and inflammatory response through ASK1 suppression in MASH [19]. In our current study, despite similar levels of liver enzymes, NAS score, and HYP were observed in HFHC groups with or without Dusp9 knockdown, the Dusp9 deficiency markedly impaired the effects of CAFF on improving hepatic inflammation and fibrosis in MASH mice, indicating Dusp9 is involved in regulating hepatic inflammatory and fibrotic progressions and its critical role of being a target of CAFF in treating MASH with early stage of liver fibrosis. Meanwhile, the suppression of ASK1-*p*38/JNK signaling by CAFF was also largely negated in Dusp9 knockdown mice, given the critical role of the ASK1-*p*38/JNK signaling pathway in mediating apoptosis, necrosis, and inflammation [37,55], the reversion of the ASK1-*p*38/JNK signaling pathway in Dusp9 knockdown mice and Dusp9 silenced hepatocytes *in vitro* strongly suggests that CAFF improves liver inflammation and fibrosis progression through MAPK signaling, with Dusp9 being a crucial mediator.

It is worth pointing out that published studies have identified that the expression and activity of Dusp9 are tightly regulated at transcriptional, and post-transcriptional levels by various factors, including the BMP4, which induces the recruitment of Smad1/5 and Smad4 to the Dusp9 promoter and activates its transcription [20,56]. Given that hepatic Dusp9 expression was markedly rescued by CAFF, it is essential to determine whether CAFF affects Dusp9 promoters or its post-transcriptional process. In addition to Dusp9, other Dusp family members, such as Dusp-7/12/26, have also been reported to influence MASLD progression [57–59], whether CAFF regulates other Dusp families remains unclear.

Of note, coffee and CAFF were proven to suppress food consumption in clinics [60,61]. In our study, CAFF presented powerful suppression on food intake in MASH mice, which explains the reversed body and liver weights, as well as ameliorated lipid and glucose metabolism in CAFF administration groups. However, the amount of food consumption is comparable in CAFF treatment groups with or without Dusp9

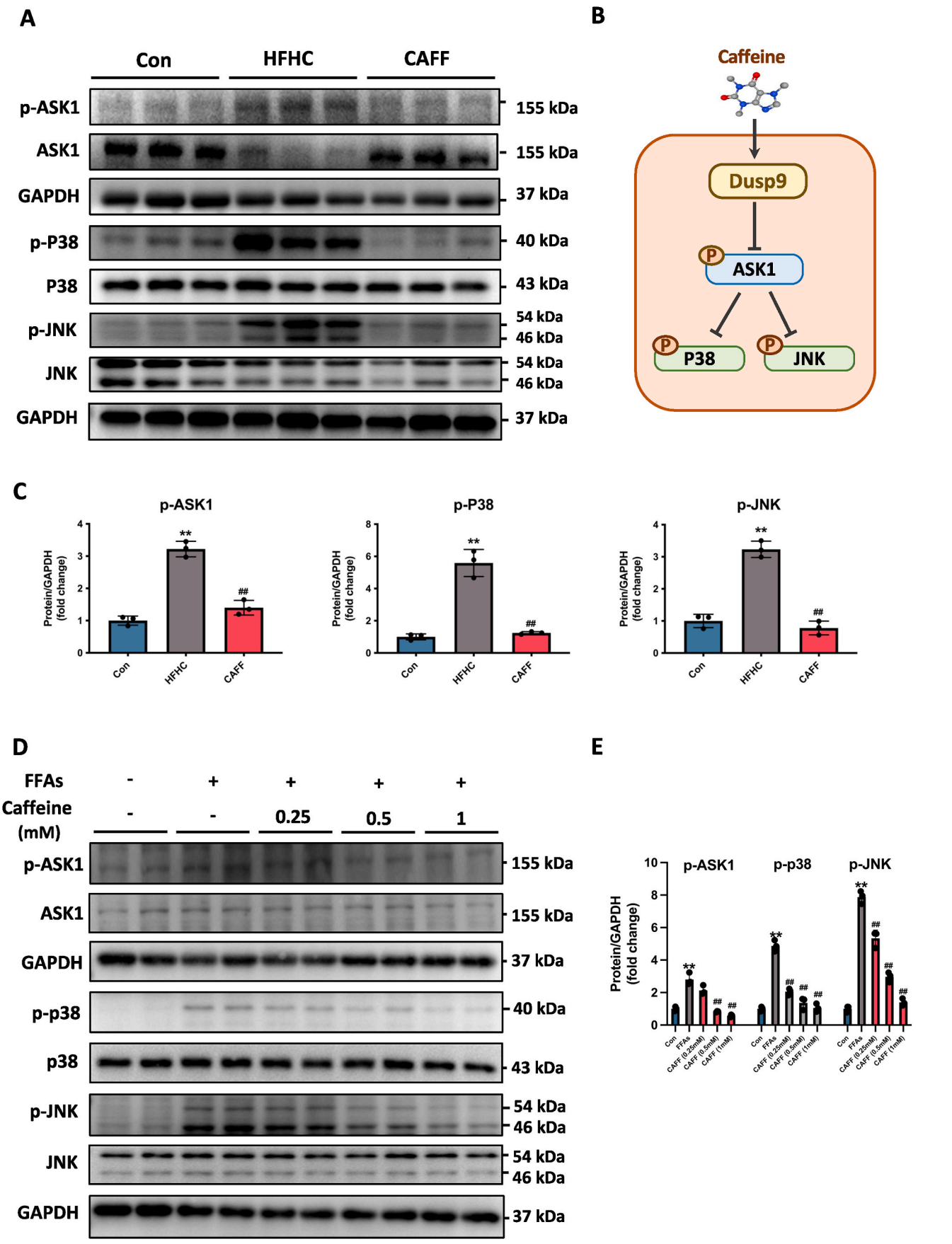

(caption on next page)

Fig. 4. Caffeine treatment inhibits MAPK signaling *in vivo* and *in vitro* MASH models. (A) Dusp9 downstream signaling kinases including hepatic p-ASK1, ASK1, p-p38, p38, *p*-JNK, and JNK, were detected with Western blot in MASH mice. (B) Schematic illustrating CAFF rescues the expression of Dusp9 attenuated by the HFHC diet and further blocks the phosphorylation of MAPK signaling. (C) Relative levels of p-ASK1, p-p38, and *p*-JNK were analyzed. (D) MAPK signaling molecules including p-ASK1, ASK1, p-p38, p38, *p*-JNK, and JNK were tested with Western blot in FFA-induced THLE-2 cells. (E) Relative levels of p-ASK1, p-p38, and *p*-JNK were analyzed in THLE-2 cells. Experiments were performed three times independently, and values represent means ± SD.*, compared with Con $p < 0.05$; **, compared with Con $p < 0.01$; #, compared with HFHC $p < 0.05$; ##, compared with HFHC $p < 0.01$. The data were analyzed with a two-sided Student's t-test or one-way ANOVA.

knockdown (Sup Fig. 5B), but Dusp9 knockdown still markedly impaired the beneficial effects of CAFF administration in MASH mice, which supports the conclusion that the therapeutic effects of CAFF are partly but dependently attributed to the hepatic Dusp9. Our previous data suggested that CAFF affects MASH via multiple signaling pathways [16]. And we also noticed that the therapeutic effects of CAFF were not entirely abolished by Dusp9 silencing, indicating incomplete hepatic Dusp9 mutation or other potential targets or mechanisms are involved. One decent study highlighted EGFR as the binding target of CAFF in treating MADLF by using SPR assay [62], supporting multiple binding targets of CAFF in treating MASLD/MASH. Moreover, a well-documented study previously showed that CAFF stimulates hepatic lipid metabolism by inducing the autophagy-lysosomal pathway [63]. Except for the influences in the liver, CAFF was reported to alleviate MASLD by stimulating IL-6 production in muscles [64], indicating CAFF presents beneficial effects on multiple organs. Insulin-HNF4α-Cyp7b1 signaling [65], and TLR4-MAPK–NF–kB signaling [66] were also indicated to be involved in treating MASLD. Collectively, these previous works support that Dusp9 is not the sole target of CAFF in treating MASLD/MASH. Moreover, except for CAFF, nutrients in other healthy beverages, such as EGCG extracted from green tea, also offer benefits for MASLD [16,67]. The effects and mechanisms of drinking healthy beverages in managing MASLD/MASH need more investigation.

In summary, the present study systematically recapitulated the multiple beneficial effects of caffeine, including ameliorated liver glycolipid metabolism, reduced liver inflammation, and fibrosis in MASH models. Using several target-identifying approaches, especially by using SPR, CETSA, and DARTS assays, Dusp9 was highlighted as one of the most critical targets strongly rescued by caffeine intervention. Furthermore, we confirmed that Dusp9 deficiency exacerbates MASH in our 36-week HFHC diet-induced MASH model. Most therapeutic effects of caffeine consumption were significantly diminished following hepatic Dusp9 knockdown *in vivo* and *in vitro*. Additionally, the expression of Dusp9-regulating signals, such as ASK1, *p*38, and JNK kinases, was tightly reversed by caffeine, ultimately suppressing the hepatic lipogenesis, inflammatory, and fibrogenic gene expression. Taken together, our study systematically demonstrated that caffeine alleviates MASH by rescuing hepatic Dusp9, which in turn controls DNL, liver inflammation, and fibrosis. Our data provided experimental evidence for the daily coffee consumption and clinical administration of caffeine-rich beverages, such as black coffee, in ameliorating MASH patients.

4. Materials & methods

4.1. Preparation of reagents

Caffeine ($C_8H_{10}N_4O_2$, molecular weight: 194.19, drug purity 99.75 %, CAS 58-08-2, lot number 200412) was purchased from Shanghai Winherb Medical Technology Co., Ltd. (Shanghai, China). The diet for the HFHC model and HFD + CCl_4 group was a 58 kcal% fat w/sucrose Surwit Diet (D12331, lot number: 1911131A10, Research Diets, USA), and the diet for the control (Con) group was an 11 kcal% fat w/cornstarch Surwit Diet (D12328, lot number: 19102112A4, Research Diets, USA). Fructose and sucrose (F0001/S0001) were purchased from Trophic Animal Feed High-Tech Co., Ltd., China. Carbon tetrachloride (10006418) and olive oil (8001-25-0) were purchased from Sinopharm Group Chemical Reagent Co., Ltd. The target sequences were designed by Invitrogen online software, and the constructed miRNAi plasmid and Dusp9 plasmid were transfected into 293T cells, and the constructed vector plasmid and adeno-associated virus packaging plasmid were co-transfected into 293T cells. Cells were collected and high titer adeno-associated virus samples were concentrated. The titer was determined by Q-PCR, an absolute quantitation method. The titer of negative control virus AAV2/8-hTBG-eGFP-miRNAi (NC) was $1.88*10^{13}$v.g./ml, and the titer of interference virus AAV2/8-hTBG-eGFP-miRNAi (Dusp9) (sequence: 5′- GCATCCGCTACATCCTCAA -3′) was $1.93*10^{13}$v.g./ml.

4.2. Animals and treatment

All animal studies were approved by the Animal Research Ethics Committee of Shanghai University of Traditional Chinese Medicine (Ethics number: PZSHUTCM200628009). All 6-week-old, wild-type, male C57BL/6 SPF mice with a body mass of 20–22 g were purchased from Shanghai SLAC Laboratory Animal Co., Ltd. and kept, modeled, and observed in a barrier-protected animal room in the animal research center at Shanghai University of Traditional Chinese Medicine (SYXK (Shanghai) 2018–0003). The mice were housed under standard conditions, with a temperature of 25 ± 2 °C and a relative humidity of 50 ± 5 %. A 12-h on/off lighting cycle was implemented using incandescent lamps. The mice were provided with ad libitum access to feed and water throughout the study.

4.2.1. HFHC diet-induced MASH mice

To observe the effect of caffeine on MASH mice, after one week of adaptation, 18C57BL/6J mice were fed with the high-trans fatty acid and high-sugar diets (D12331 diet and sugar water 42 g/L, fructose: sucrose 55 %: 45 %) were fed for 30 weeks to establish a MASH model [21], and the control group was fed with a normal chow diet and tap water. At the beginning of modeling, the mice were randomly divided into the control group (Con, n = 8) and a high-fat and high-glucose group (HFHC, n = 16). After 30 weeks of modeling, the HFHC mice were divided into the HFHC group and CAFF group according to body weight. The CAFF group was given Caffeine dissolved in drinking water (75 mg/kg) by gavage, while the Con and HFHC groups were given the drinking water by gavage for 6 weeks.

4.2.2. HFHC combined with CCl_4 injection-induced MASH mice with liver fibrosis

To observe the effect of caffeine on MASH mice with liver fibrosis, after one week of adaptation, C57BL/6J mice were fed with the above HFHC diet and intraperitoneally injected with 10 % CCl_4-olive oil solution (2 ml/kg) for 6 weeks. The control group was fed with the above control diet. At the end of the second week of modeling, the MASH mice were divided into the HFHC group and CAFF group. The CAFF group was given caffeine dissolved in drinking water (75 mg/kg) by gavage, while the Con and HFHC groups were given drinking water by gavage for 4 weeks.

4.2.3. Dusp9 knockdown mice

To establish a Dusp9 knockdown mouse model, a pre-test of Dusp9 knockdown efficiency was performed: At the end of 26 weeks of high-fat and high-carbohydrate diet modeling, 12 mice were injected with adeno-associated virus by tail vein injection of 0.1ml/mouse, and the model was established by continued high-fat and high-carbohydrate diet for 4 weeks. At the end of 30 weeks, the mice were sacrificed. Western blot was used to verify the Dusp9 expression. In the formal experiment:

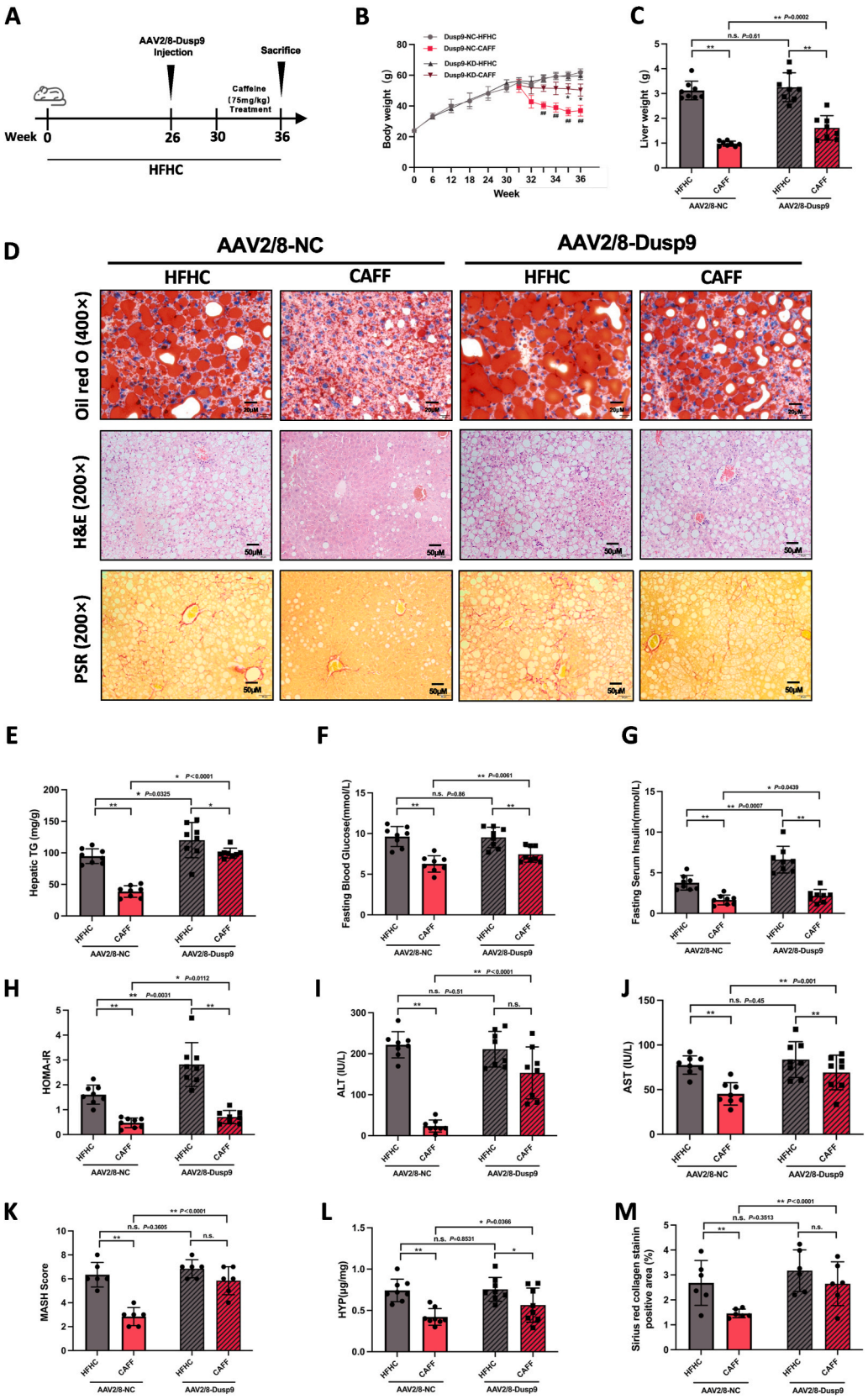

Fig. 5. Liver-specific Dusp9 knockdown exacerbates glycolipid metabolism and abolishes caffeine-mediated multiple amelioration in MASH mice. (A) The flow chart shows administration modeling, tail vein injection of AAV, administration, and sacrifice time point (n = 8, per group). (B–C) Body weight and liver weight. (D) Representative images showed Oil red O, H&E, and PSR staining from indicated groups; PSR quantification is analyzed in (M). (E) Hepatic TG contents (mg/g) in each group. (F–H) Fasting plasma glucose, fasting insulin, and insulin resistance index (HOMA-IR) in each group. (I–J) Serum ALT and AST activities. (K) Hepatic MASH score (MASH activity score) in each group. (L) Hydroxyproline content of liver tissue in each group (n = 8, per group). Values represent means ± SD.*$p <$ 0.05; **$p < 0.01$; n. s. = no significance. The data were analyzed with a two-sided Student's t-test or one-way ANOVA.

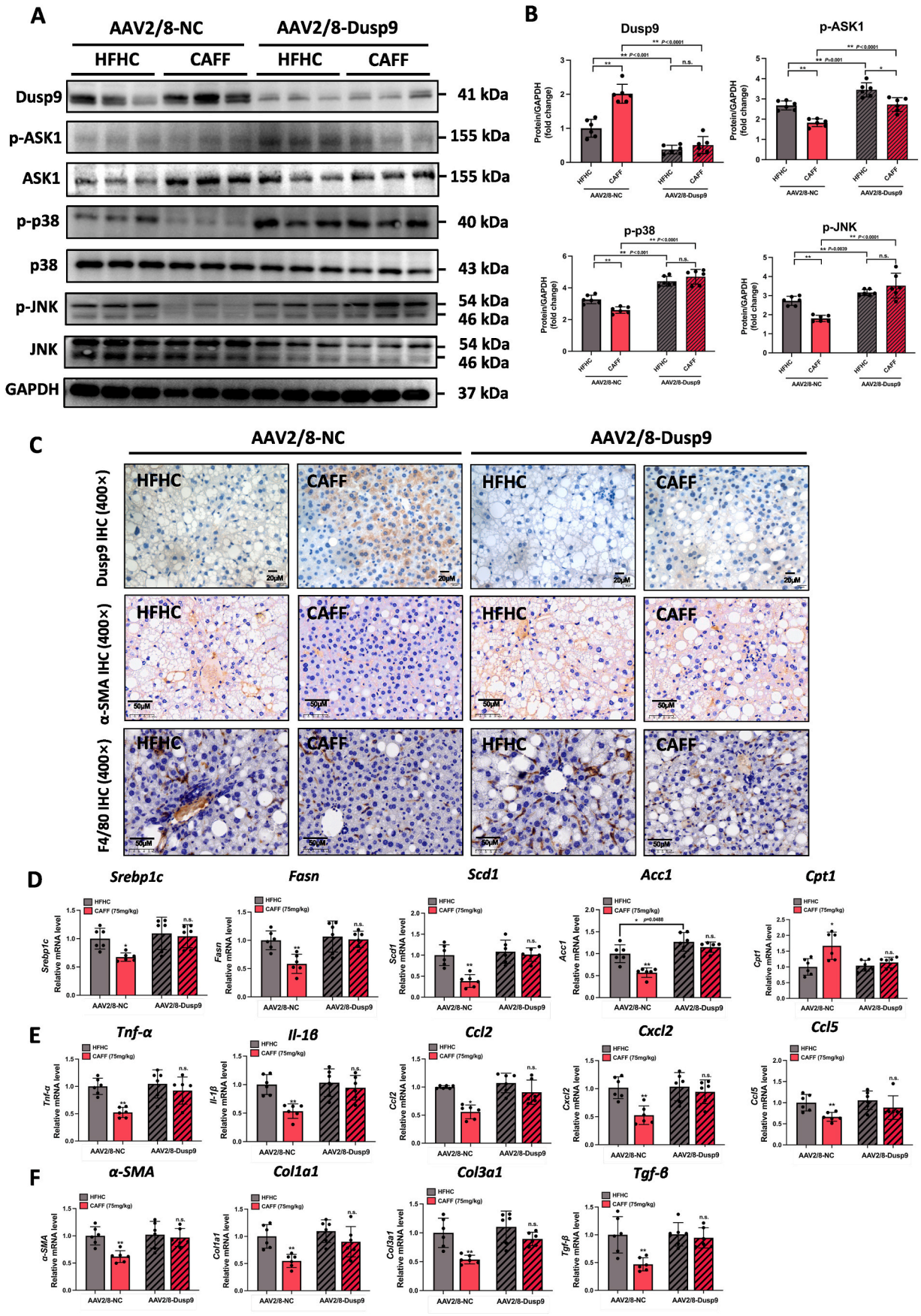

(caption on next page)

Fig. 6. Dusp9 knockdown activates MAPK signaling, exacerbates liver inflammation and fibrosis, and diminishes the protective effects of caffeine in MASH mice. (A) Expression levels of hepatic Dusp9, p-ASK1, ASK1, p-p38, p38, *p*-JNK, and JNK protein were examined with Western blot in HFHC NASH mice. (B) Western blot data of relative expression of Dusp9, p-ASK1, p-p38, and *p*-JNK protein in HFHC NASH mice. (C) Immunohistochemical detection of Dusp9, α-SMA, and F4/80 (brown/tan) and nuclei (blue) in liver tissue from HFHC-fed NASH mice. (D) Quantitative PCR analysis of hepatic mRNA levels of genes related to lipid metabolism (*Srebp1c, Fasn, Scd1, Acc1,* and *Cpt1a*) in the indicated groups. (E) Quantitative PCR analysis of hepatic mRNA levels of genes related to inflammation (*Tnf-α, Il-1β, Ccl2, Cxcl2*, and *Ccl5*) in the indicated groups. (F) Quantitative PCR was performed to determine the hepatic mRNA levels of genes related to fibrosis (*α-SMA, Col1a1, Col3a1,* and *Tgf-β*) in the indicated groups. Experiments were performed three times independently, and values represent means ± SD.*, compared with Con $p < 0.05$; **, compared with Con $p < 0.01$; #, compared with HFHC $p < 0.05$; ##, compared with HFHC $p < 0.01$. The data were analyzed with a two-sided Student's t-test or one-way ANOVA.

at the end of 26-week modeling, 32 mice were injected with AAV2/8-hTBG-eGFP-miRNAi negative control (NC) virus or AAV2/8-hTBG-eGFP-miRNAi (Dusp9) virus, 16 mice per each group. Mice from two groups were further randomly divided into the HFHC group and the CAFF group (n = 8). All the above groups were given CAFF drugs or drinking water by gavage for 6 weeks. The method of injection of Dusp9 adeno-associated virus was as follows: the liver was the target organ, and the injection volume was generally 100 μl (0.1 ml). The amount of virus injected per mouse was generally 1–2 $*10^{11}$ V. g. The required volume of virus stock solution for each mouse was 10 μl, and the total volume of fluid was injected into the tail vein of each mouse: 10 μl (virus stock solution) +100 μl (PBS buffer/saline). According to the virus packaging, 500 μl (PBS buffer/saline) was added to each tube of 50 μl virus stock. The mice were fixed on the mouse fixator to expose the tail, and the tail of the mice was heated evenly with a heating lamp. The best injection site was found in the order from the tail tip to the tail root for injection.

4.3. Cell culture and treatment

The human liver cell line (THLE-2) [29] was purchased from Shanghai Institute of Life Sciences. They were cultured in bronchial epithelial cell basal medium and additives (BEGM from Lonza/Clonetics Corporation, USA, BEGM Bullet Kit; CC3,170). 1.5×10^5 cells were seeded in a six-well plate for all experiments. Cells were tested for mycoplasma contamination. DMSO was used to prepare caffeine cell drugs (0.25 mM, 0.5 mM and 1 mM). Experiments were started when the cells had grown to 60–70 % confluence. Steatosis was induced by culturing FFAs (oleic (0.5 mM) and palmitic acid (0.25 mM) in a 2:1 ratio) in cells supplemented with 10 % FBS for 24 h. The cells were divided into the control group (Con), FFA group (FFAs), and FFA+0.25–1 mM group (FFAs+0.25 mM, FFAs+0.5 mM, FFAs+1 mM). After additional incubation with the corresponding drugs for 24 h, TG was detected, stained with Oil red O, and imaged. The cytotoxicity of Caffeine was detected by the CCK-8 kit (Sigma, 96992).

4.4. Construction of lentivirus and cell transfection

All lentiviral constructs were prepared by Shanghai Genechem Co., LTD. (Shanghai, China). Lentiviral adshRNA-Dusp9 transfection was performed according to the manufacturer's instructions. In general, THLE-2 cells were infected with AdshRNA-Dusp9 or control lentivirus (AdshRNA-NC). Lentiviral vectors and packaging plasmids were mixed and transfected into THLE-2 cells using Lipofectamine 2000 (Invitrogen Life Technologies, Carlsbad, CA, USA). After 6–8 h of culture, the virus was removed and replaced with fresh medium.

4.5. SPR assay

The binding kinetics or affinity of Caffeine with DUSP9 (ZY60716HuP)was assessed via SPR using a Biacore T200 instrument and manufacturer-provided software (GE Healthcare), and all measurements were performed at 25 °C. The CM7 chips were activated with 75 mg/mL *N*-(3-dimethylaminopropyl)-*N*′-ethylcarbodiimide hydrochloride and 10 mg/mL *N*-hydroxysuccinimide. Dusp9 was diluted to 10 μg/ml with 10 mmol/L sodium acetate (pH 5.0), and then covalently immobilized on CM7 chips by amino coupling. The protein coupling solutions were injected over the activated CM7 chip surface to achieve an immobilization level of about 10,000 resonance units (RU), and a blank surface which was similarly treated but without immobilization with PGAM5 protein solutions was used as a reference surface flow cell. The coupling procedure was run at the flow rate of 10 μL/min. Binding kinetics or affinity measurements were performed at a flow rate of 30 μL/min using PBS-P+ buffer, and the running parameters were 90 s of binding with compound or DMSO solution, 90 s of dissociation with PBS-P+ buffer, and 180 s of regeneration with Glycine-HCl (pH 1.5) buffer. The values of RU responses were recorded, and sensor grams were processed and analyzed using Biacore T200 control and evaluation software and the binding curves were fitted to determine the equilibrium dissociation constant (KD).

4.6. Cellular thermal shift assay (CETSA)

As previously described [68], briefly, cells were cultured for 1 day with fresh medium on the 10-cm plate. On the test day, cells were exposed to the indicated concentration of compounds (1 mM Caffeine) for the specified time (120 min). The control group was incubated with an equal volume of DMSO. Following incubation, the cells were washed with PBS to remove excess Caffeine/DMSO. The suspension was centrifuged at 340 g and 25 °C for 5 min, washed twice with PBS, and diluted with PBS to 100 million cells/ml. After this, they were subjected to a 3-min heat shock to the appropriate heat cycle (42–63 °C) for generating melt curves followed by rapid cooling to 25 °C. Then the cells were lysed in liquid nitrogen for 3 min through three freeze-thaw cycles. Centrifuge the pelleted proteins and cell debris at 11,800 g for 20 min to make pellets. Transfer the supernatant to gel loading buffer and analyze protein levels with Western blot.

4.7. Drug affinity responsive target stability (DARTS)

Drug affinity Response target Stability (darts) is a commonly used method to identify small-molecule protein interactions. The principle is that the protease sensitivity of the target protein decreases after drug binding. Because it does not require modification of the drug and does not depend on the mechanism of action of the drug, it has universal applicability. THLE-2 cells were lysed with RIPA supplemented with protease and phosphatase inhibitors for 30 min. Dimethyl sulfoxide (DMSO) or different concentrations of Caffeine (0.25,0.5,1 mM) were added to the cell lysates and incubated for 60min at room temperature. At the end of the incubation period, the samples were divided into 20 μL for later use. 2 μL of protease solution was added to the sample tube (the appropriate protease concentration was pre-determined, protease: protein = 1:500), and 2 μL buffer was added to the control group. The cells were incubated for 15 min at room temperature, and protease inhibitor solution was added to each sample, mixed, and frozen for 10 min to stop proteolysis. Finally, 6 μL of 5 x electrophoresis sample buffer was added to verify the binding of Dusp9 to Caffeine by analyzing the expression of the target protein by western blotting.

4.8. Specimen collection

All mice were fasted 12h before the end of the experiment and

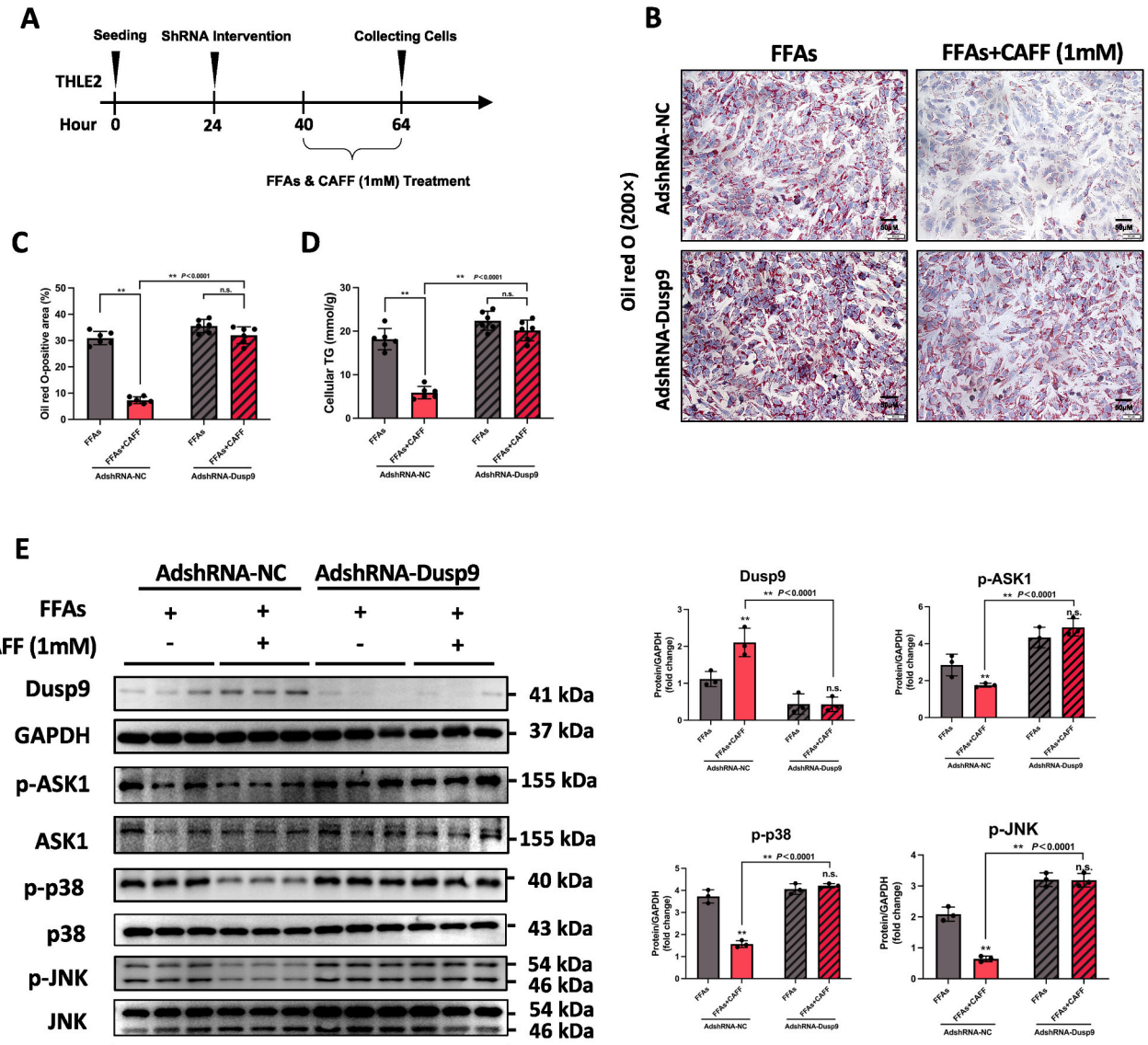

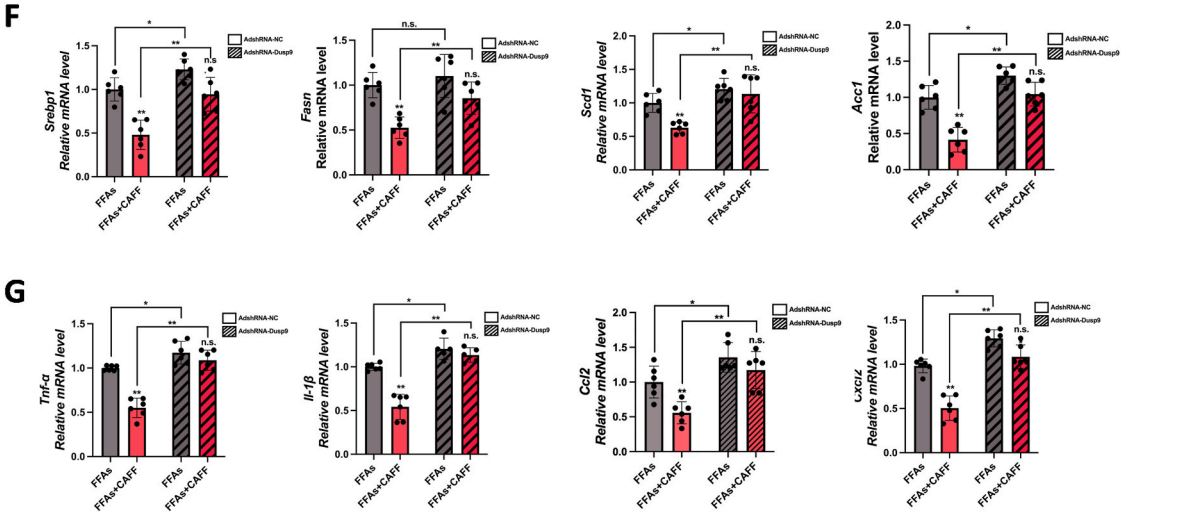

(caption on next page)

Fig. 7. Dusp9 silencing impairs the effects of caffeine on lipid accumulation, inflammation, and MAPK signaling in FFA-induced THLE-2 cells. (A) Flow chart illustrating the experimental design for Dusp9 silencing by lentiviral transfection, followed by FFAs and CAFF incubation. The experiment was repeated three times. (B, C) Representative pictures showed Oil red O staining and semi-quantitative assessment of Oil red O content. Scale bar, 20 μm (n = 3 independent experiments per group). (D) Levels of TGs in THLE-2 cells in the indicated groups. (E) Dusp9 downstream signaling molecules including p-ASK1, ASK1, p-p38, p38, *p*-JNK, and JNK were tested with Western blot in FFA-induced THLE-2 cells. Relative levels of p-ASK1, p-p38, and *p*-JNK were analyzed in THLE-2 cells. (F) Quantitative PCR was performed to determine the hepatic mRNA levels of genes related to lipid metabolism (*Srebp1, Fasn, Scd1,* and *Acc1*) in the indicated groups. (G) Quantitative PCR was performed to determine the hepatic mRNA levels of genes related to inflammation (*Tnf-α, Il-1β, Ccl2,* and *Cxcl2*) in the indicated groups. Experiments were performed three times independently, and values represent means ± SD.*, compared with Con $p < 0.05$; **, compared with Con $p < 0.01$; #, compared with HFHC $p < 0.05$; ##, compared with HFHC $p < 0.01$. The data were analyzed with a two-sided Student's t-test or one-way ANOVA.

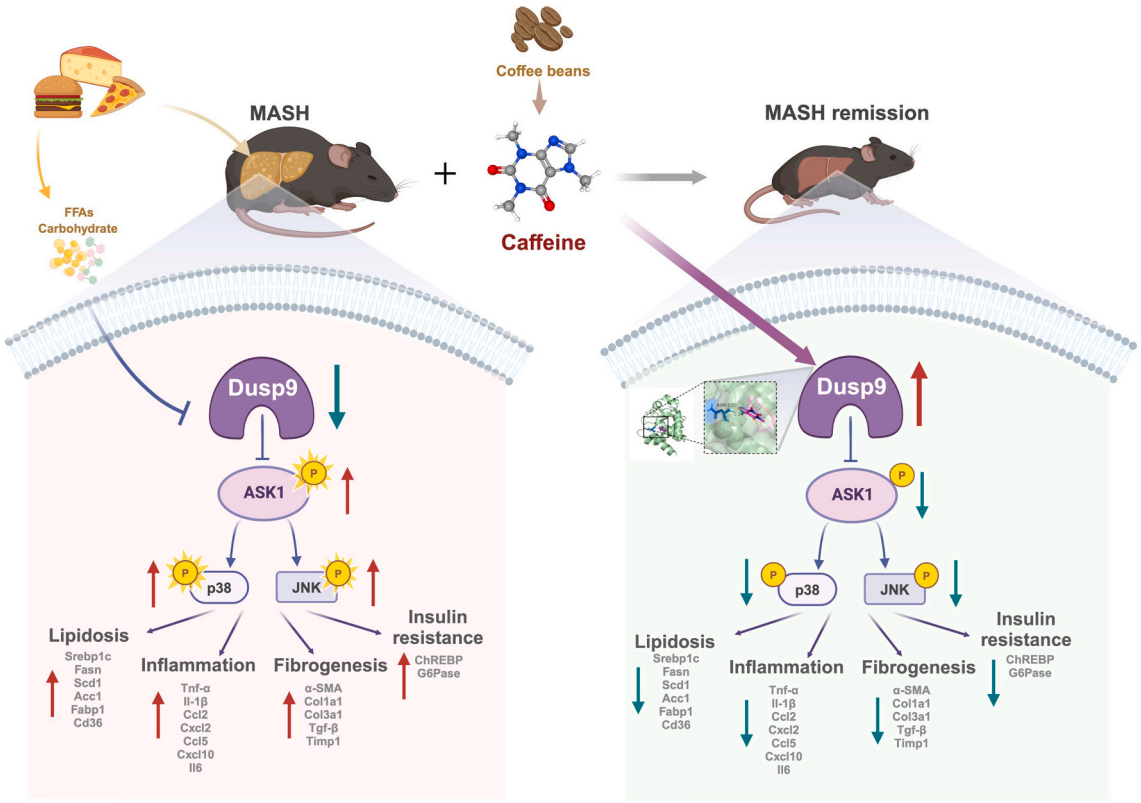

Fig. 8. A schematic overview depicting the ameliorative effects of caffeine on MASH through rescuing impaired Dusp9 and inactivating MAPK pathway. Caffeine (CAFF) is Caffeine (CAFF), the most abundant natural component in coffee beans, ameliorates metabolic-associated steatohepatitis (MASH) by enhancing glycolipid metabolism, reducing inflammation, and reversing liver fibrosis. Impairment of Dusp9 due to long-term HFHC diet feeding leads to the phosphorylation and activation of the MAPK pathway, which drives the progression of MASH. However, CAFF administration rescues the impaired Dusp9 and inhibits its downstream signaling activation, representing a critical mechanism and therapeutic target for improving MASH.

anesthetized by intraperitoneal injection of 2 % sodium pentobarbital 3 ml/kg 1 ml of blood was collected from each mouse. A portion of liver tissue was extracted from the same liver lobe, placed at the same location in each mouse, and fixed in a 10 % neutral buffered formalin solution.

4.9. Serum biochemical assays

Serum ALT and aspartate aminotransferase (AST) activities were measured using ALT and AST assay kits (Lot number 20180628, Nanjing Jiancheng Bioengineering Institute, Nanjing, China). To assess glucose metabolism, mice were fasted for 12 h, after which 3 μL of blood was collected from the tail vein, and fasting blood glucose (FBG) was measured using a Roche blood glucose meter (Roche Diagnostic GmbH, Germany). Fasting insulin (FINS) levels in the serum of mice from each group were measured using an enzyme-linked immunosorbent assay (Ultra-Sensitive Mouse Insulin ELISA Kit, lot number: 90080, Crystal Chem, USA). The homeostatic model assessment-insulin resistance (HOMAIR) index was calculated using the following formula: FBG (mM) × FINS (IU/L)/22.5.

4.10. Hepatic biochemical assays

Hepatic TG content was measured using a kit (A0-10017, Dong'ou Diagnostic Products Co. Ltd., Zhejiang, China), and hepatic hydroxyproline (HYP) content was measured using an HYP assay kit (D126, Nanjing Jiancheng Bioengineering Institute, Nanjing, China), as previously described [21].

4.11. Histological examination and assessment

Fixed liver tissue was dehydrated and embedded using a tissue processor (Leica ASP300) and a paraffin embedding station (Leica EG1160). Then, the sections were stained using a hematoxylin and eosin (H&E) staining kit (lot number 20200625, Nanjing Jiancheng Bioengineering) and a Sirius Red Staining Kit (lot number 20200528, Nanjing Jiancheng Bioengineering). Liver tissue was fixed in liquid nitrogen, embedded in ornithine carbamoyl transferase medium, and sectioned at −20 °C at a thickness of 10 μm. The sections were stained using an Oil Red O staining kit (lot number 20200430, Nanjing Jiancheng Bioengineering), as described previously. The NASH Activity Score (NAS) is a

semi-quantitative scale to predict NASH. A NAS score of <3 can be used to exclude NASH, a score >4 can be used to diagnose NASH, and a score of 3–4 indicates possible NASH. The higher the score, the more active the lesion, and the higher the degree of hepatic steatosis. Fibrosis staging was used to determine the degree of fibrosis in the liver tissue. The fibrosis stages were scored from F0 to F4, as follows: F0, no fibrosis; F1, perisinusoidal or periportal fibrosis; F2, perisinusoidal and portal fibrosis without bridging formation; F3, bridging fibrosis and nodules; and F4, cirrhosis. Image Pro Plus was used to calculate the positive area of the Sirius Redstained and Masson-stained images. Eight visual fields were taken from each image to calculate the area of liver fibrosis.

4.12. Western blot analysis

Liver tissue or cells were homogenized in lysis buffer (150 mM NaCl, 1 % Nonidet P-40, 0.1 % SDS, 50 mM Tris-HCl pH 7.4, 1 mM EDTA, 1 mM PMSF, and 1 × Roche complete mini protease inhibitor cocktail). The supernatants were collected after centrifugation at 10,000×*g* at 4 °C for 15 min. Protein concentration was determined using a BCA protein assay kit (Beyotime Institute of Biotechnology, Jiangsu, China). Equal amounts of protein were separated by 10 % SDS gel electrophoresis under denaturing and non-reducing conditions and transferred to a polyvinylidene difluoride membrane. The membrane was blocked with 5 % nonfat milk in TBST at room temperature for 1 h and then incubated with the appropriate primary antibody at 4 °C overnight (antibody information is presented in Supplementary Table 1). After three washes in TBST, the blots were incubated with horseradish peroxide-coupled secondary antibody. The signals were visualized using an enhanced chemiluminescence system (Pierce Biotechnology, Inc., Rockford, IL, USA) and recorded in a chemiluminescence imaging system (ChemiScope 3500 mini, Qin Xiang, China).

4.13. Immunohistochemistry (IHC)

Samples were first incubated in anti-α-SMA antibody at a dilution of 1:100 (α-SMA, 1:100, catalog number: ab5694, USA) overnight at 4 °C and then incubated with primary antibody at a dilution of 1:250. Some liver sections were also stained with anti-Col-I antibody (Col-I, Abcam, 1:100, ab34710, USA), anti-F4/80 antibody (F4/80, CST, 1:1000, 70076, USA), and anti-DUSP9 antibody (DUSP9, CST, 1:1000, 45914, USA) using the same method.

4.14. Reverse transcription polymerase chain reaction (RT-PCR)

Total RNA isolated was subjected to RT-PCR with an RNA PCR kit (RNA extraction: Sangon Biotech (Shanghai) Co., Ltd. B511321; RNA reverse transcription: BioRad, 1708890) for determining mRNA levels of genes in Supplementary Table 2. Nucleotide sequences of the PCR primers are shown in the figure below. In brief, the PCR conditions for reverse transcription are 25 °C for 5 min, 46 °C for 20 min, and 95 °C for 1 min, for 50 cycles. The RT-PCR products were resolved via agarose gel electrophoresis and stained with 1 % ethidium bromide.

4.15. Library preparation and Illumina HiSeq X ten sequencing

Libraries were size selected for cDNA target fragments of 200–300 bp on 2 % Low Range Ultra Agarose, followed by PCR amplification using Phusion DNA polymerase (NEB) for 15 PCR cycles. After quantification with a TBS380 fluorometer, the paired-end RNA-seq sequencing library was sequenced with an Illumina HiSeq X Ten sequencing system (2 × 150 bp read length). The data were GSEA analyzed using the free online Majorbio ISanger Cloud Platform (www.i-sanger.com).

4.16. Target prediction and molecular docking

To predict the target of Caffeine, the webserver PharmMapper (http://lilab-ecust.cn/pharmmapper/) was used [69]. The potential targets of MASH were acquired from Genecards (https://www.genecards.org/). For molecular docking, the molecular structure of Caffeine, Dusp9, Col1a1, Ccl2, and Cd68 was acquired from PubChem (https://pubchem.ncbi.nlm.nih.gov/) and PROTEIN DATA BANK (https://www.rcsb.org/).To test the binding affinity of Caffeine on Dusp9, Col1a1, Ccl2, and Cd68, we used the molecule visual software Chimera 1.16 and Auto Dock VINA. Automatic docking VINZA is a set of automatic docking tools. It is widely used to predict small molecules, such as drug candidates. The docking score is based on the Auto Dock VINA score. 2D visualization of docking pose is using visual software Discovery Studio 2020.

4.17. Statistical analysis

Statistical analysis of database data was performed using SPSS 24.0 software for Mac OS. The measurement data in the statistical description are indicated by S and refer to the count data. When the normality and homogeneity of the variance were satisfied, a Student t-test was applied for comparison of the two groups. Data from multiple groups were compared with one-way ANOVA or two-way ANOVA analysis followed by Tukey's post hoc test. The comparison of the hierarchical grouping data was calculated via Radit analysis. To show the dispersion of the samples, all statistical results are presented as Mean ± SD.

CRediT authorship contribution statement

Xin Xin: Writing – review & editing, Writing – original draft, Visualization, Validation, Supervision, Project administration, Methodology, Investigation, Formal analysis, Conceptualization. **Cheng Chen:** Writing – review & editing, Writing – original draft, Supervision, Project administration, Methodology, Formal analysis, Data curation, Conceptualization. **Xiao Xu:** Validation, Methodology. **Sheng Lv:** Validation, Methodology. **Qinmei Sun:** Validation, Investigation. **Ziming An:** Validation, Methodology. **Yi Chen:** Software, Methodology, Investigation. **Zhekun Xiong:** Supervision, Project administration. **Yiyang Hu:** Writing – review & editing, Visualization, Supervision, Data curation, Conceptualization. **Qin Feng:** Writing – review & editing, Validation, Supervision, Project administration, Methodology, Investigation, Formal analysis, Data curation, Conceptualization.

Ethics statement

The animal study was reviewed and approved by the Animal Studies Ethics Committee of Shanghai University of Traditional Chinese Medicine.

Funding statement

This work was supported by National Science Foundation of China (No.82174040 to Q. F., No. 82405138 to X.X., No. 82174186 to Y·H.); Shanghai Sailing Program (No. 23YF1448200 to X.X.); SIMM-SHUTCM Traditional Chinese Medicine Innovation Joint Research Program (2022, E2G807H).

Declaration of competing interest

The authors disclose no conflicts of interest.

Acknowledgements

We thank Dr. Dingqi Zhang (Shanghai University of TCM) and Rong Hong (Shanghai Nanfang Model Biotechnology Co., LTD) for providing technical assistance.

Appendix A. Supplementary data

Supplementary data to this article can be found online at https://doi.org/10.1016/j.redox.2025.103499.

Data availability

Data will be made available on request.

References

[1] J.V. Lazarus, et al., Advancing the global public health agenda for NAFLD: a consensus statement, Nat. Rev. Gastroenterol. Hepatol. 19 (1) (2022) 60–78.
[2] Z.M. Younossi, et al., The global epidemiology of nonalcoholic fatty liver disease (NAFLD) and nonalcoholic steatohepatitis (NASH): a systematic review, Hepatology 77 (4) (2023) 1335–1347.
[3] T.C. Yip, et al., Asian perspective on NAFLD-associated HCC, J. Hepatol. 76 (3) (2022) 726–734.
[4] G. Targher, et al., The complex link between NAFLD and type 2 diabetes mellitus - mechanisms and treatments, Nat. Rev. Gastroenterol. Hepatol. 18 (9) (2021) 599–612.
[5] E. En Li Cho, et al., Global prevalence of non-alcoholic fatty liver disease in type 2 diabetes mellitus: an updated systematic review and meta-analysis, Gut 72 (11) (2023) 2138–2148.
[6] O.O. Badmus, et al., Molecular mechanisms of metabolic associated fatty liver disease (MASLD): functional analysis of lipid metabolism pathways, Clin. Sci. (Lond.) 136 (18) (2022) 1347–1366.
[7] Y. Sakurai, et al., Role of insulin resistance in MASLD, Int. J. Mol. Sci. 22 (8) (2021).
[8] D. Ferguson, B.N. Finck, Emerging therapeutic approaches for the treatment of NAFLD and type 2 diabetes mellitus, Nat. Rev. Endocrinol. 17 (8) (2021) 484–495.
[9] N. Eshaghian, et al., Sugar sweetened beverages, natural fruit juices, and cancer: what we know and what still needs to be assessed, Front. Nutr. 10 (2023) 1301335.
[10] J. Chhimwal, V. Patial, Y. Padwad, Beverages and Non-alcoholic fatty liver disease (NAFLD): think before you drink, Clin Nutr 40 (5) (2021) 2508–2519.
[11] V.W. Setiawan, et al., Association of coffee intake with reduced incidence of liver cancer and death from chronic liver disease in the US multiethnic cohort, Gastroenterology 148 (1) (2015) 118–125, quiz e15.
[12] M. Romero-Gomez, S. Zelber-Sagi, M. Trenell, Treatment of NAFLD with diet, physical activity and exercise, J. Hepatol. 67 (4) (2017) 829–846.
[13] J.W. Molloy, et al., Association of coffee and caffeine consumption with fatty liver disease, nonalcoholic steatohepatitis, and degree of hepatic fibrosis, Hepatology 55 (2) (2012) 429–436.
[14] M. Ding, et al., Caffeinated and decaffeinated coffee consumption and risk of type 2 diabetes: a systematic review and a dose-response meta-analysis, Diabetes Care 37 (2) (2014) 569–586.
[15] F. Shang, X. Li, X. Jiang, Coffee consumption and risk of the metabolic syndrome: a meta-analysis, Diabetes Metab. 42 (2) (2016) 80–87.
[16] X. Xin, et al., Caffeine and EGCG alleviate high-trans fatty acid and high-carbohydrate diet-induced NASH in mice: commonality and specificity, Front. Nutr. 8 (2021) 784354.
[17] H. Xu, et al., Dual specificity mitogen-activated protein (MAP) kinase phosphatase-4 plays a potential role in insulin resistance, J. Biol. Chem. 278 (32) (2003) 30187–30192.
[18] B. Emanuelli, et al., Overexpression of the dual-specificity phosphatase MKP-4/DUSP-9 protects against stress-induced insulin resistance, Proc. Natl. Acad. Sci. USA 105 (9) (2008) 3545–3550.
[19] P. Ye, et al., Dual-specificity phosphatase 9 protects against nonalcoholic fatty liver disease in mice through ASK1 suppression, Hepatology 69 (1) (2019) 76–93.
[20] F.Z. Khoubai, C.F. Grosset, DUSP9, a dual-specificity phosphatase with a key role in cell biology and human diseases, Int. J. Mol. Sci. 22 (21) (2021).
[21] X. Xin, et al., High-trans fatty acid and high-sugar diets can cause mice with non-alcoholic steatohepatitis with liver fibrosis and potential pathogenesis, Nutr. Metab. 17 (2020) 40.
[22] M.V. Machado, H. Cortez-Pinto, NAFLD, MASLD and obesity: brothers in arms? Nat. Rev. Gastroenterol. Hepatol. 20 (2) (2023) 67–68.
[23] I.R. Schlaepfer, M. Joshi, CPT1A-mediated fat oxidation, mechanisms, and therapeutic potential, Endocrinology 161 (2) (2020).
[24] P. Rada, et al., Understanding lipotoxicity in NAFLD pathogenesis: is CD36 a key driver? Cell Death Dis. 11 (9) (2020) 802.
[25] M.E. Miquilena-Colina, et al., Hepatic fatty acid translocase CD36 upregulation is associated with insulin resistance, hyperinsulinaemia and increased steatosis in non-alcoholic steatohepatitis and chronic hepatitis C, Gut 60 (10) (2011) 1394–1402.
[26] T. Mukai, et al., Silencing of FABP 1 ameliorates hepatic steatosis, inflammation, and oxidative stress in mice with nonalcoholic fatty liver disease, FEBS open bio 7 (7) (2017) 1009–1016.
[27] M.A. Herman, et al., A novel ChREBP isoform in adipose tissue regulates systemic glucose metabolism, Nature 484 (7394) (2012) 333–338.
[28] J.N. Clore, J. Stillman, H. Sugerman, Glucose-6-phosphatase flux in vitro is increased in type 2 diabetes, Diabetes 49 (6) (2000) 969–974.
[29] S. Sefried, et al., Suitability of hepatocyte cell lines HepG2, AML12 and THLE-2 for investigation of insulin signalling and hepatokine gene expression, Open Biol 8 (10) (2018).
[30] K. Tomita, et al., CXCL10-Mediates macrophage, but not other innate immune cells-associated inflammation in murine nonalcoholic steatohepatitis, Sci. Rep. 6 (2016) 28786.
[31] K. Kazankov, et al., The role of macrophages in nonalcoholic fatty liver disease and nonalcoholic steatohepatitis, Nat. Rev. Gastroenterol. Hepatol. 16 (3) (2019) 145–159.
[32] L. Malaguarnera, et al., Chitotriosidase gene expression in Kupffer cells from patients with non-alcoholic fatty liver disease, Gut 55 (9) (2006) 1313–1320.
[33] T.L. Bissoondial, et al., Liver biopsy hydroxyproline content is a diagnostic for hepatocellular carcinoma in murine models of nonalcoholic steatohepatitis, Diagnostics 10 (10) (2020).
[34] S.G. Patching, Surface plasmon resonance spectroscopy for characterisation of membrane protein-ligand interactions and its potential for drug discovery, Biochim. Biophys. Acta 1838 (1 Pt A) (2014) 43–55.
[35] T. Jiang, et al., Arbutin alleviates fatty liver by inhibiting ferroptosis via FTO/SLC7A11 pathway, Redox Biol. 68 (2023) 102963.
[36] S. Schuster, A.E. Feldstein, NASH: novel therapeutic strategies targeting ASK1 in NASH, Nat. Rev. Gastroenterol. Hepatol. 14 (6) (2017) 329–330.
[37] M. Xiang, et al., Targeting hepatic TRAF1-ASK1 signaling to improve inflammation, insulin resistance, and hepatic steatosis, J. Hepatol. 64 (6) (2016) 1365–1377.
[38] S.A. Harrison, et al., A phase 3, randomized, controlled trial of resmetirom in NASH with liver fibrosis, N. Engl. J. Med. 390 (6) (2024) 497–509.
[39] S.A. Harrison, et al., Resmetirom for nonalcoholic fatty liver disease: a randomized, double-blind, placebo-controlled phase 3 trial, Nat Med 29 (11) (2023) 2919–2928.
[40] M. Kokkorakis, et al., Resmetirom, the first approved drug for the management of metabolic dysfunction-associated steatohepatitis: trials, opportunities, and challenges, Metabolism 154 (2024) 155835.
[41] F. Asgari-Taee, et al., Association of sugar sweetened beverages consumption with non-alcoholic fatty liver disease: a systematic review and meta-analysis, Eur. J. Nutr. 58 (2019) 1759–1769.
[42] E.G. de Mejia, M.V. Ramirez-Mares, Impact of caffeine and coffee on our health, Trends Endocrinol. Metabol. 25 (10) (2014) 489–492.
[43] R. Anty, et al., Regular coffee but not espresso drinking is protective against fibrosis in a cohort mainly composed of morbidly obese European women with NAFLD undergoing bariatric surgery, J. Hepatol. 57 (5) (2012) 1090–1096.
[44] H. Shen, et al., Association between caffeine consumption and nonalcoholic fatty liver disease: a systemic review and meta-analysis, Therap Adv Gastroenterol 9 (1) (2016) 113–120.
[45] R. Nevola, et al., GLP-1 receptor agonists in non-alcoholic fatty liver disease: current evidence and future perspectives, Int. J. Mol. Sci. 24 (2) (2023).
[46] M.S. Westerterp-Plantenga, M.P. Lejeune, E.M. Kovacs, Body weight loss and weight maintenance in relation to habitual caffeine intake and green tea supplementation, Obes. Res. 13 (7) (2005) 1195–1204.
[47] R.M. van Dam, E.J. Feskens, Coffee consumption and risk of type 2 diabetes mellitus, Lancet 360 (9344) (2002) 1477–1478.
[48] A. Mansour, et al., Effects of supplementation with main coffee components including caffeine and/or chlorogenic acid on hepatic, metabolic, and inflammatory indices in patients with non-alcoholic fatty liver disease and type 2 diabetes: a randomized, double-blind, placebo-controlled, clinical trial, Nutr. J. 20 (1) (2021) 35.
[49] C. Kositamongkol, et al., Beverage consumption in patients with metabolic syndrome and its association with non-alcoholic fatty liver disease: a cross-sectional study, Front. Nutr. 11 (2024).
[50] Y.P. Chen, et al., A systematic review and a dose-response meta-analysis of coffee dose and nonalcoholic fatty liver disease, Clin Nutr 38 (6) (2019) 2552–2557.
[51] B. Emanuelli, et al., Overexpression of the dual-specificity phosphatase MKP-4/DUSP-9 protects against stress-induced insulin resistance, Proc Natl Acad Sci U S A 105 (9) (2008) 3545–3550.
[52] T. Wang, C. Ma, The hepatic macrophage pool in NASH, Cell. Mol. Immunol. 18 (8) (2021) 2059–2060.
[53] J. Arauz, et al., Caffeine prevents experimental liver fibrosis by blocking the expression of TGF-beta, Eur. J. Gastroenterol. Hepatol. 26 (2) (2014) 164–173.
[54] Q. Wang, et al., Caffeine protects against alcohol-induced liver fibrosis by dampening the cAMP/PKA/CREB pathway in rat hepatic stellate cells, Int. Immunopharm. 25 (2) (2015) 340–352.
[55] Q. Chen, et al., Mechanism of ASK1 involvement in liver diseases and related potential therapeutic targets: a critical pathway molecule worth investigating, J. Gastroenterol. Hepatol. 38 (3) (2023) 378–385.
[56] Z. Li, et al., BMP4 Signaling Acts via dual-specificity phosphatase 9 to control ERK activity in mouse embryonic stem cells, Cell Stem Cell 10 (2) (2012) 171–182.
[57] L. Wu, et al., Targeting DUSP7 signaling alleviates hepatic steatosis, inflammation and oxidative stress in high fat diet (HFD)-fed mice via suppression of TAK1, Free Radic. Biol. Med. 153 (2020) 140–158.
[58] Z. Huang, et al., Dual specificity phosphatase 12 regulates hepatic lipid metabolism through inhibition of the lipogenesis and apoptosis signal-regulating kinase 1 pathways, Hepatology 70 (4) (2019) 1099–1118.
[59] P. Ye, et al., Dual-specificity phosphatase 26 protects against nonalcoholic fatty liver disease in mice through transforming growth factor beta-activated kinase 1 suppression, Hepatology 69 (5) (2019) 1946–1964.
[60] A. Jessen, et al., The appetite-suppressant effect of nicotine is enhanced by caffeine, Diabetes Obes. Metabol. 7 (4) (2005) 327–333.

[61] A. Gavrieli, et al., Effect of different amounts of coffee on dietary intake and appetite of normal-weight and overweight/obese individuals, Obesity 21 (6) (2013) 1127–1132.
[62] Y.W. Huang, et al., Caffeine can alleviate non-alcoholic fatty liver disease by augmenting LDLR expression via targeting EGFR, Food Funct. 14 (7) (2023) 3269–3278.
[63] R.A. Sinha, et al., Caffeine stimulates hepatic lipid metabolism by the autophagy-lysosomal pathway in mice, Hepatology 59 (4) (2014) 1366–1380.
[64] C. Fang, et al., Caffeine-stimulated muscle IL-6 mediates alleviation of non-alcoholic fatty liver disease, Biochimica et Biophysica Acta (BBA)-Molecular and Cell Biology of Lipids 1864 (3) (2019) 271–280.
[65] G. Kakiyama, et al., Coffee modulates insulin-hepatocyte nuclear factor-4alpha-Cyp7b1 pathway and reduces oxysterol-driven liver toxicity in a nonalcoholic fatty liver disease mouse model, Am. J. Physiol. Gastrointest. Liver Physiol. 323 (5) (2022) G488–G500.
[66] E.E. Vargas-Pozada, et al., Caffeine inhibits NLRP3 inflammasome activation by downregulating TLR4/MAPK/NF-kappaB signaling pathway in an experimental NASH model, Int. J. Mol. Sci. 23 (17) (2022).
[67] C. Chen, et al., Potential biological effects of (-)-Epigallocatechin-3-gallate on the treatment of nonalcoholic fatty liver disease, Mol. Nutr. Food Res. 62 (1) (2018).
[68] A. Kawatkar, et al., CETSA beyond soluble targets: a broad application to multipass transmembrane proteins, ACS Chem. Biol. 14 (9) (2019) 1913–1920.
[69] X. Wang, et al., PharmMapper 2017 update: a web server for potential drug target identification with a comprehensive target pharmacophore database, Nucleic Acids Res. 45 (W1) (2017) W356–W360.